

CHALMERS



Management of Active Distribution Networks with High Penetration of Distributed Generation

Master's Thesis in Electric Power Engineering

AHMED ARRAM

Department of Energy and Environment
Division of Electric Power Engineering
CHALMERS UNIVERSITY OF TECHNOLOGY
Gothenburg, Sweden 2012

Master's Thesis in Electric Power Engineering

Management of Active Distribution Networks with
High Penetration of Distributed Generation

Master's Thesis in Electric Power Engineering

AHMED ARRAM

Department of Energy and Environment
Division of Electric Power Engineering
CHALMERS UNIVERSITY OF TECHNOLOGY

Gothenburg, Sweden 2012

Management of Active Distribution Networks with High Penetration of Distributed Generation

Master's Thesis in Electric Power Engineering

© AHMED ARRAM, 2012

Department of Energy and Environment
Division of Electric Power Engineering
Chalmers University of Technology
SE-412 96 Göteborg
Sweden

Abstract

The penetration of distributed generation and wind power in particular is expected to increase significantly over the coming years, and a huge shift in control, operation and planning of distribution networks is going to be necessary if this generation is to be connected in a cost effective manner. Traditionally, distribution networks have been operated as passive networks with uni-directional power flows and were designed through deterministic (load flow) studies considering the critical cases so that distribution networks could operate with a minimum amount of control. With the connection of increasing amounts of distributed generation, these networks are becoming active and with power flowing in the two directions, hence requiring more intelligent forms of management. Increasing connection of intermittent distributed generation, such as wind power, to distribution networks requires new control strategies to provide greater flexibility and use of existing network assets. Active network management (ANM) will play a major role in this and will help in facilitating connection of new generation without the need for traditional reinforcements.

This thesis is based on a multi-period AC optimal power flow (OPF)-based technique for evaluating the maximum capacity of new intermittent distributed generation able to be connected to a distribution network when ANM control strategies are in place. The ANM schemes embedded into the OPF include coordinated voltage control, adaptive power factor, energy curtailment and demand side management. A generic U.K. medium voltage distribution network is analyzed using coincident demand and wind availability data derived from hourly time-series. Results clearly show that very high penetration levels of new variable generation capacity can be achieved by considering ANM strategies compared to the widely used passive operation (i.e., “fit and forget”). It has been shown that with coordinated voltage control (CVC) there will be a positive impact on minimizing the losses in a distribution network compared with old passive operation by around 20%. Also active network management (ANM) can result in reducing the total average voltage deviation. The thesis has founded that the DG installed capacity can be increased by active network schemes to some extent in case of load growth.

Keywords: distributed generation, passive operation, active network management, multi period AC optimal power flow, coordinated voltage control, adaptive power factor control, energy curtailment, demand side management.

Acknowledgement

Many people have been a part of my graduate education, as friends, teachers, colleagues and family. I would like to dedicate this work, this thesis, to them. Their inspiration has kept me going through this amazing stage of my academic career.

First and foremost, I wish to offer my sincerest gratitude to my advisor, Dr. Tuan Le at the Department of Energy and the Environment and Chalmers University of Technology. I am very grateful for his keen supervision, advice, technical facilities and assistance throughout the entire thesis process; without which I would never have succeeded.

I would also like to thank Lindo Systems for giving me a full license to use their software, Lingo v.13. I used its optimization capabilities in many of the computations in this thesis.

I would also like to thank Prof. Gareth P. Harrison, Dr. Luis F. Ochoa and my cool brother, Mahmoud Arram for lending their support, via eloquent emails, throughout this work.

And most of all, my parents and brother, who made it possible for me to be here in the first place, and have always stood by me. This work is for you.

Sincerely yours,

Ahmed Arram

Goteborg, July 2012

Table of Contents

Abstract.....	i
Acknowledgement	iii
List of Tables	vi
List of Figures	vii
List of Symbols and Abbreviations:	viii
Chapter 1 Introduction	1
1.1 Background	1
1.2 Motivation and problem statement:.....	1
1.3 Scope of the thesis.....	4
1.4 Organization of the thesis.....	5
Chapter 2 Literature Review	7
2.1 Distributed generation definition:	7
2.2 Maximizing the DG capacity:	7
2.3 Minimizing the energy losses and maximizing the difference between the renewable energy and the energy losses.....	10
2.4 The demand side management DSM	11
2.5 Summary:	11
Chapter 3 Problem Formulation with Multi-Period AC Optimal Power Flow.....	13
3.1 Mathematical representation of a long distribution cable:	13
3.2 Multi-Period AC OPF model (base case or passive management):	14
3.2.1 Objective Function:	14
3.2.2 Constraints:.....	14
3.3 Incorporating Active Network Management.....	18
3.3.1 Coordinated Voltage Control.....	18
3.3.2 Adaptive Power Factor Control (PFc) or Coordinated Generator Reactive Power Control.....	19
3.3.3 Energy Curtailment.....	20
3.3.4 Demand Side Management DSM:.....	22
Chapter 4 : Case Study, Simplified EHV1 Network-Single DG	25
4.1 Study Case	25
4.1.1 Data and assumptions	25
4.1.2 Load data and wind power data:.....	26
4.1.3 Network Data.....	27
4.2 Results and Analysis of the Study Case:	28
4.2.1 Comparison between two study cases using graphs	30
4.3 Results and Analysis in Case of using DSM:.....	38
Chapter 5 : Other Objective Functions and Load Growth Consideration.....	41
5.1 Minimizing the Losses	41
5.1.1 Introduction:	41
5.1.2 Formulating the Energy Loss Minimization Problem Using A Multi-period AC Optimal Power Flow:	41
5.2 Trade-off between energy losses and renewable Energy	43
5.3 Minimizing the Total Average Voltage Deviation.....	45
5.4 Studying the effect of load growth	46

Chapter 6 : Conclusions and Future Works:	49
6.1 Conclusions:	49
6.2 Future Work:	49
Appendices.....	51
A.1: Classification of Optimization Problems	51
A.2:”Proof of power flow equations”	51
A.3: Data of the Simplified EHV1 Network from the U.K. Generic Distribution System (GDS)	53
A.4: Data entry and implementation of case study of maximizing the DG capacity	58
A.5: Implementation.....	60
A.7: Unknown Variables	64
References:.....	66

List of Tables

Table 4-1: Coincident hours for each of the demand/generation scenarios [6].	26
Table 4-2: The 20 different scenarios/cases, where cases A, B and C represent passive operation and the other cases are active management cases.	27
Table 4-3: The 20 different cases and their maximum DG capacity.	29
Table 4-4: The main differences between the 20 different cases:	37
Table 5-1: Minimization of total energy losses and the 8 different cases.	43
Table A-1: Classification of optimization problems according to difficulty	51
Table A-2: Buses of the simplified EHV1 network.	53
Table A-3: Generators of the EHV1 simplified network.	54
Table A-4: branches of the simplified EHV1 Network:	54
Table A-5: Transformers of the simplified EHV1 network.	55
Table A-6: Peak active and reactive Load at each bus of the simplified EHV1 Network	57
Table A-7: Percent of peak demand and percent of generation capacity during each period.	58
Table A-8: Values of Conductance, susceptance, shunt susceptance and line limits	59
Table A-9: Peak active and reactive power at each bus in the EHV1 network:	59

List of Figures

Figure 3-1: Pi Model of a line.....	13
Figure 4-1: (Top) Winter and (bottom) Summer hourly demand and wind power production (relative to peak) for central Scotland, 2003[44].Two different wind profiles are considered:WP1(black line) and WP2(grey line).....	25
Figure 4-2: coincident hours for each of the demand/generation scenarios [6].....	26
Figure 4-3:U.K. GDS simplified EHV1 network at maximum load [6].....	27
Figure 4-4: Simplified EHV1 network: connectable DG capacity (in MW) with ANM strategies (capacitive, i: inductive, and PFC: adaptive power factor control).29	
Figure 4-5: Tapping position for OLTC and VR together with the secondary voltage of both OLTC and VR for case D.....	31
Figure 4-6: Tapping position of the OLTC & VR for case T	32
Figure 4-7: Secondary voltage of OLTC & VR for case T.....	32
Figure 4-8: Voltage magnitude at bus 12 for case D.	33
Figure 4-9: Voltage magnitude at bus 12 for case T.....	33
Figure 4-10: Reactive power support at bus 2 and bus 9 for case D	34
Figure 4-11: Extra reactive power support at bus 2 for case T.....	34
Figure 4-12: Active power curtailed in case T.....	35
Figure 4-13: DG active power injection in both cases (D & T).....	36
Figure 4-14: Slack bus active power injection in both cases.	36
Figure 4-15: Losses in MWh in case of maximizing the DG capacity.	37
Figure 4-16: Maximum DG capacity in case of using DSM using Random Demand Curtailment factor at bus b during each certain period m	40
Figure 4-17: Max DG Capacity in case of using DSM with random demand curtailment factor at bus b and fixed for all periods.	40
Figure 5-1: The minimum active energy losses.....	42
Figure 5-2: The corresponding DG capacity when the objective is to minimize the losses.	43
Figure 5-3: Net maximum (Renewable energy –losses) in MWH.	44
Figure 5-4: The corresponding DG capacity in case of maximizing the (Renewable energy – losses)	45
Figure 5-5: Minimum average voltage deviation.....	46
Figure 5-6: Maximum DG capacity for load increase by 7%.....	48
Figure 5-7: Maximum DG capacity for a load increase by 14%.	48

List of Symbols and Abbreviations:

DG	Distributed Generation.
OLTC	On Line Tap Changer.
VR	Voltage Regulator.
$PF_{g,m}$	Power factor at generator bus g during period m .
PF_g^-	Lower limit of power factor at generator bus g .
PF_g^+	Upper limit of power factor at generator bus g .
PFC	Power Factor Control (taken between 0.95 inductive to 0.98 inductive).
ANM	Active Network Management.
DNO	Distribution Network Operators.
DSM	Demand Side Management.
CVC	Coordinated Voltage Control.
m	Index of the period.
M	Set of total existing periods (indexed by m).
g	Index of the number of Generators.
p_g	Distributed generation Capacity of generator g .
G	Set of total generators (indexed by g).
b	Index of Bus.
B	Total number of buses.
V_b^-	Lower limit voltage of bus b .
V_b^+	Maximum limit voltage of bus b .
$V_{b,m}$	Voltage at bus b during period m .
l	Index of Lines.
L	Total number of lines.
$f_{l,m}^{1,P}$	Active power injection onto line l at the start of the bus and during period m .
$f_{l,m}^{2,P}$	Active power injection onto line l at the end of the bus and during period m .
$f_{l,m}^{1,Q}$	Reactive power injection onto line l at the start of the bus and during period m .
$f_{l,m}^{2,Q}$	Reactive Power injection onto line l at the end of the bus and during period m .
f_l^+	The apparent power flow limit on line l .
g_l	Conductance of line l .
b_l	Susceptance of line l .
β_l^1	Starting bus of line l .

β_l^2	Ending bus of line l .
$V_{\beta_{l,m}^1}$	Voltage at the starting bus of line l and during period m .
$V_{\beta_{l,m}^2}$	Voltage at the ending bus of line l and during period m .
$\delta_{\beta_{l,m}^1}$	Voltage angle at the starting bus of line l and during period m .
$\delta_{\beta_{l,m}^2}$	Voltage angle at the ending bus of line l and during period m .
t_{OLTC}^-	The minimum tap position of the OLTC as a per unit nominal value.
$t_{OLTC,m}^+$	The maximum tap position of the OLTC as a per unit nominal value.
t_{VR}^-	The minimum tap position of the VR as a per unit nominal value.
t_{VR}^+	The maximum tap position of the VR as a per unit nominal value.
$T_{OLTC,m}$	The tap position of the OLTC as a per unit nominal value during period m .
$T_{VR,m}$	The tap position of the VR as a per unit nominal value during period m .
d_b^P	Peak active power demand at bus b .
d_b^Q	Peak reactive power demand at bus b .
η_m	Demand level relative to peak demand during period m .
w_m	Generation level relative to nominal generation capacity during period m .
$p_{x,m}$	Exported power by external connection from external source x during period m .
$q_{x,m}$	Exported reactive power by external connection from external source x during period m .
x	Index of external sources.
X	Set of external sources.
β_x	Location of external source x .
β_g	Location of distributed generator g .
b_l^C	Shunt Capacitance of line l .
$\phi_{g,m}$	Power angle of distributed generator during period m .
ϕ_g^-	Minimum limit of power angle of distributed generator.
ϕ_g^+	Maximum limit of power angle of distributed generator.
p_x^-	Minimum active power supplied by external source x .
p_x^+	Maximum active power supplied by external source x .
$p_{x,m}$	Active power supplied by external source x during period m .
q_x^-	Minimum reactive power supplied by external source x .
q_x^+	Maximum reactive power supplied by external source x .
$q_{x,m}$	Reactive power supplied by external source x during period m .
bo	Slack bus.

$\delta_{bo,m}$	Slack bus voltage angle during period m .
$V_{b_{OLTC}}^-$	Lower limit voltage of the secondary bus of the OLTC.
$V_{b_{OLTC},m}$	Voltage at secondary bus of the OLTC during period m .
$V_{b_{OLTC}}^+$	Upper limit voltage of the secondary bus of the OLTC.
$V_{b_{V.R}}^-$	Lower limit voltage of the secondary bus of the VR.
$V_{b_{V.R},m}$	Voltage at secondary bus of the VR during period m .
$V_{b_{V.R}}^+$	Upper limit voltage of the secondary bus of the VR.
$p_{g,m}^{curt}$	Power curtailed at generator bus g during period m .
τ_m	Duration of period m in hours.
λ_{curt}	Curtailement factor.
$V_{b,nominal}$	Nominal voltage at bus b .
$dP_{b,m}^{curtail}$	Active demand power curtailed at load bus b during certain period m .
f^{min}	Lower limit of a random number.
$f_{b,m}$	Random Demand Curtailement factor at bus b during certain period m .
f^{max}	Upper limit of a random number.
$Q_{b,m}^C$	External reactive power support at bus b during period m , there is $Q_{2,m}^C$ & $Q_{9,m}^C$ only.
r_l	Series resistance of the line l .
x_l	Series reactance of the line l .
z_l	Series impedance of the line l .
y_l	Admittance of line l .
$S_{l,m}^1$	Complex power at the start of line l during period m .
$S_{l,m}^2$	Complex power at the end of line l during period m .
$dP_{b,m}$	Active power demand at bus b during period m .
$dQ_{b,m}$	Reactive power demand at bus b during period m .
$dP_{b,m}^{curtail}$	Active power demand curtailed at bus b during period m .
$dQ_{b,m}^{curtail}$	Reactive power demand curtailed at bus b during period m .

1

Introduction

This chapter presents the difference between passive and active distribution networks, discusses the benefits of active management of distribution systems. The chapter also discusses the main problems that face distribution network operators (DNO) when they aim to increase the DG penetration in the existing distribution networks. This chapter shows the aims, scope, limitation, and organization of this thesis.

1.1 Background

Distributed generation is an electric power source connected directly to the distribution network or on the customer site of the meter [1].

The penetration of distributed generation and wind power in particular is expected to increase significantly over the coming years, and a huge shift in control, operation and planning of distribution networks is going to be necessary if this generation is to be connected in a cost effective manner.

Traditionally, distribution networks have been operated as passive networks with uni-directional power flows and were designed through deterministic (load flow) studies considering the critical cases so that distribution networks could operate with a minimum amount of control. With the connection of increasing amounts of distributed generation, these networks are becoming active and with power flowing in the two directions, hence requiring more intelligent forms of management.

The transition from passively to actively managed distribution networks is driven by [2] :

- Government environmental commitments to connect a large number of small-scale generation plants.
- Technological advances in energy generation and storage as well as in information and communication technologies.
- Regulatory reform and unbundling of energy industry.

The practice of passive operation of distribution networks can limit the capacity of the distributed generation that can be connected to an existing system.

In contrast, active management techniques enable the distribution network operator to maximize the use of the existing circuits by taking full advantage of control of transformer taps, voltage regulators, reactive power management [2], demand side management and system reconfiguration in an integrated manner (this thesis will not discuss system reconfiguration).

1.2 Motivation and problem statement:

The main function of an electrical power system is to transport electrical power from the generators to the loads. In order to function properly, it is essential that the voltage is kept

close to the nominal value, in the entire power system. Traditionally, this is achieved differently for transmission networks and for distribution grids. In transmission networks, the large scale centralized power plants keep the node voltages within the allowed deviation from their nominal values and the number of dedicated voltage control devices is limited [2]. Distribution grids, in contrast, incorporate dedicated equipment for voltage control and the generators connected to the distributed generation are hardly involved in controlling the node voltages.

The traditional (passive operation) approach has been challenged by recent developments; one of these is the increased use of wind turbines for generating electricity connected to distribution grids. They affect the currents, or the power flows, in the distribution grid to which they are connected, and, because node voltages are strongly related to power flows, they also change node voltages [2]. This can lead to problems if the devices installed in the distribution grid cannot compensate the impact of wind turbines on node voltages. In this case the, the voltages at some nodes within the distribution grid cannot be kept within the allowed deviation from their nominal value, and appropriate measures have to be taken.

A similar problem arises when the large scale wind farms are connected to the transmission network. Again the wind farm affects the power flows and hence the node voltages, but this time in the transmission network. Here, voltages are controlled mainly by large scale conventional power plants. If their capability is not sufficient to compensate the impact of the wind farm on the node voltages, again, the voltages at some nodes can no longer be kept within the allowable deviation from its nominal value and appropriate measures has have to be taken.

The wind power will have an impact on the voltage control, on transmission (beyond the scope of this thesis) and on distribution grids.

As branches have a capacitance, resistance and inductance, a current flowing through a branch causes a voltage difference between the ends of the branch (i.e. between the nodes being connected by the branch). However, even though there is a voltage difference between the two ends of the branch, the node voltage is not allowed to deviate from the nominal value of the voltage in excess of a certain value (normally 5% to 10%) [2] and throughout this thesis it is fixed at 6%. Appropriate measures must be taken to prevent such deviation. Voltage control refers to the task of keeping the node voltages in the system within the required limits and of preventing any deviation from the nominal value to become larger than allowed.

It is also important to stress that node voltage is a local quantity, as opposed to system frequency, which is a global or quantity so it is impossible to control the voltage at a certain node from any point in the system. Instead, the voltage of a certain node can be controlled only at that particular node or in its direct vicinity.

There are various ways to affect node voltages. They differ fundamentally between transmission networks and distribution grids. This is because of the different characteristics of the branches in transmission networks and distribution grids as

transmission systems have low R/X ratio while distribution grids have a high R/X ratio [2].

Traditionally, the two most important approaches towards voltage control in distribution grids are:

- The use of tap-changing transformers (i.e. transformers in which the turns ratio can be changed).
- Devices that can generate or consume reactive power (i.e. shunt capacitors or reactors).

The whole voltage profile of the distribution grid is shifted up or down by using tap-changing transformers, depending on whether the transformer turns ratio is decreased or increased. While capacitors and reactors perform better in this respect, because they affect mainly the voltage of the node to which they are connected. However, the sensitivity of the node voltage to changes in reactive power is rather limited and therefore relatively large capacitors and reactors are necessary. This disadvantage is due to the high R/X ratio of the branches in distribution grids when compared with that in transmission networks as mentioned before.

More and more distributed generation such as wind turbines is being connected to distribution grids. These generators affect the power flows in distribution grids. In particular, if their output power does not correlate with the load, as is the case with generators using an uncontrollable prime mover, such as wind, the variations in the current through the branches and therefore in the node voltages increase. The maximum and minimum value of the current through a certain branch used to depend on the load only, but, with the connection of distributed generation, the current limits have become dependent on the load as well as on the output of the distributed generator. The limits are now determined by a situation with minimum generation and maximum load, on one hand, and maximum generation and minimum load on the other, rather than only by the difference between minimum and maximum load, as used to be the case.

A fundamental feature of the passive networks is their inability to accommodate increased amounts of DG, and it was demonstrated that the voltage rise effect is the main limiting factor for connecting DG's in distribution and rural areas, the voltage rise effect can be effectively controlled within an active network environment and as a result, enable considerably higher levels of penetration of DG to be connected into existing systems.

The ability of active networks to accommodate DG will be illustrated through use of a United Kingdom distribution network as a case study. It will be shown that the amount of DG that can be connected to the existing distribution network can be increased significantly by changing the operating philosophy from active to passive and this thesis tries to give answers to the following questions:

- What are the potential benefits of changing the operation philosophy of distribution network and embedded wind generation from passive to active management?
- What is the best control strategy (or combined control strategy) for an existing distribution network which facilitates connection of new generation without the need for traditional reinforcement?
- How to build a model, based on multi-period AC optimal power flow that maximizes the capacity of the distributed generation or minimize the losses when active network management control strategies are in place?
- What is the benefit of using a multi-period AC power technique in evaluating network capacity for accommodating intermittent distributed generation DG compared with the snapshot approach?
- What is the practical limitation capability of the optimization software available to solve a large non-linear problem?

1.3 Scope of the thesis

In this thesis, a multi-period AC optimal power flow technique will be used for showing the benefits of applying active management in existing distribution networks in:

- Increasing the amount of DG capacity significantly that can be connected to the existing distribution network can be increased significantly by changing the operating philosophy from active to passive while respecting the operation constraints such as voltage statutory limits and distribution lines thermal limits.
- Reducing the network losses significantly by changing the operating philosophy from active to passive while respecting the operation constraints such as voltage statutory limits and distribution lines thermal limits.
- Maximizing the difference between the renewable energy and losses while respecting the operation constraints such as voltage statutory limits and distribution lines thermal limits.
- Minimizing the average voltage deviation in order to reduce the frequent operation of the taps of the OLTC (On Load Tap Changer) and voltage regulator in the active distribution network while respecting the operation constraints such as voltage statutory limits and distribution lines thermal limits.

The entire above four main points will be achieved through implementing four main control strategies, which are:

- Coordinated voltage control of OLTC and voltage regulators.
- Adaptive power factor control
- Energy Curtailment.
- Demand side management, which will be only used to maximize the DG capacity.

1.4 Organization of the thesis

The organization of this thesis is as described below:

Chapter 1 shows the difference between passive and active distribution networks, discusses the benefits of active management of distribution systems and why it is important, also focuses on the main problem that faces the DNO (distribution network operators) when they aim to increase the DG penetration to existing distribution networks, and finally it shows the scope and limitation of this study work and what is its aim.

Chapter 2 covers as much as possible of the scientific research papers published regarding this thesis.

Chapter 3: describes a basic multi-period AC OPF for maximizing the total active DG capacity is formulated in mathematical form and four active management schemes are incorporated and described, these active management schemes are:

- Coordinated Voltage Control (CVC)
- Adaptive Power Factor Control (PFc)
- Energy Curtailment.
- Demand Side Management (DSM).

Chapter 4 covers the application of the different active management schemes to a simplified EHV1 Network from the U.K. Generic Distribution System in order to maximize the DG capacity of a connected wind farm, the DSM active management scheme will also be applied to the same generic distribution system and the results will be analyzed separately at the end of the same chapter.

Chapter 5 uses the same simplified network used in chapter 4 as a case study for applying different multi period AC OPF with each having three different objective functions, these objective functions are:

- Minimizing the losses.
- Trade-off between energy losses and renewable energy, the objective function aim is to maximize the renewable energy from the DG and reduce the distribution network losses at the same time.
- Minimizing the total average voltage deviation.

In addition to that, a separate study on the effect of load growth on the future DG capacity.

Management of Active Distribution Networks with High Penetration of Distributed Generation

2

Literature Review

This chapter defines distributed generation and includes a literature review of up to date research papers regarding the topics covered in this thesis

2.1 Distributed generation definition:

Distributed generation (DG) refers to power generation at the point of consumption, generating power on-site, rather than centrally and according to the CIGRE Working Group 37.23[3] definition, which characterizes dispersed generation as:

- Not centrally planned
- Today not centrally dispatched
- Usually connected to the distribution network
- Smaller than 50 or 100 MW

Not centrally planned or dispatched means that major influences such as unit commitment or reactive power generation are out of control of the system operator.”

2.2 Maximizing the DG capacity:

In reference [4], passive distribution network operating philosophy tends to limit the amount of EWG that can be connected into the distribution network. [4] demonstrates the benefits of alternative active network controls such as generation curtailment, reactive power absorption and coordinated OLTC (on-load-tap-control), for voltage regulation within an existing distribution network. It was shown that by implementing active network management, the increase in installed capacity of EWG (Embedded wind generation) which can be connected to the existing distribution networks can be increased considerably, as shown in the examples, especially that using coordinated OLTC control). Advanced optimal power flow (OPF) was developed to investigate the potential benefits and cost of the proposed controls.

In reference [4], a given level of penetration of EWG (embedded wind generation), OPF (optimal power flow) calculations are performed over a horizon of one year for the following three alternative control strategies:

- Embedded wind generation EMG curtailment during low load.
- Reactive power management using a reactive compensator.
- Area based on load tap changer coordinated voltage control.

The modeling of the hourly output of the wind generation is based on Stochastic Markov model based on [5], this model is used to create a normalized annual generation profile, which was a bases for constructing wind generator output for various installed capacities, and the increase in EWG (embedded wind generation) penetration using the above alternative controls was investigated using optimal power flow (OPF). A linear

programming (LP) based formulation of the OPF is selected, and an algorithm composed of different steps has to be followed during each iteration [4].

In [4], the objective function is to minimize the annual active generation curtailment cost, while satisfying the voltage limits and thermal constraints and determining the value of the corresponding controls applied such as:

- Curtailment of active and reactive generation needed at the DG bus and at time t .
- Reactive power absorbed by a reactive compensator at time t .
- Tap setting of the tap-changer at time t .

In [4], the objective function was to minimize the annual active generation curtailment cost through a linear programming (LP) based formulation of the OPF and an algorithm composed of different steps during each iteration and this thesis did not study that case with the objective function of “minimizing the annual active generation curtailment cost”, but all the conclusions in [4] are consistent with the conclusions in this thesis.

So it can be said that this thesis applies a novel, flexible multi-period AC OPF based technique exactly as in [6] while [4] uses a linear technique as mentioned before.

Firm connection would require that the DG capacity be restricted despite the opportunity for much higher energy production. The alternative is a “non-firm” connection wherein the DNO (distribution system operator) may curtail the output of the renewable DG at low demand [4],[7]; this allows connection of larger DG generators but at the expense of lost production [4].

ANM (active network management) has not yet been deployed widely due to regulatory and commercial barriers [8],[9]. In part this is due to a need to justify investment in control and communications infrastructure in terms of the benefits to the DNO and wider stakeholders [6].

Schemes such as coordinated voltage control, dynamic ratings, power factor control and automatic restoration can improve the controllability and reliability of the distribution network [4, 7, 10-12], but this thesis doesn't study the effect of ANM (active network management) on distribution network reliability as this is beyond the scope of this thesis.

The problem of adequately, or “optimally”, siting and sizing DG units has become the focus of a number of studies. Using techniques ranging from impact indexes [13-15], this thesis focuses on the optimal sizing of the DG units and does not use impact indexes and siting of the DG units is beyond the scope of this thesis.

In [13] the impact indexes used for siting and sizing of the DG units are:

- Voltage profile improvement index.
- Line loss reduction index.
- Environmental impact reduction index.
- DG benefit index.

In [14] a multi-objective performance index that relates impact indices by strategically assigning a relevance factor to each index is proposed.

In [15], it is shown that load models can significantly affect the optimal location and sizing of DG resources in distribution systems, the effect of load models on the sizing of the DG is not in interest of this thesis and also the optimal location of the DG is also beyond this thesis scope.

In [16], the problem of adequately, or “optimally”, siting and sizing DG units using analytical approaches such as multi-objective performance index that relates impact indices by strategically assigning a weighting factor to each index was proposed. A number of impact indices were addressed in the paper, aimed at characterizing the benefits and negative impacts of DG in distribution networks. More impact indices, such as reliability, economics and environmental concerns can be included in the procedure but nonetheless would add complexity.

C. Wang in [17] focuses on the proper location of DGs in power systems to obtain their maximum potential benefits. The paper presents analytical methods to determine the optimal location to place a DG in radial as well as networked systems to minimize the power loss of the system.

An algorithm based on analytical approach is to calculate the optimum size of DG at various buses and proposes a fast methodology to identify the best location corresponding to the optimum size for reducing total power losses in primary distribution network is presented in [18].

The problem of adequately, or “optimally”, siting and sizing DG units has become the focus of a number of studies using metaheuristics methods with an implemented technique based on a genetic algorithm [19-21], or linear methods such as in [4], [22], and nonlinear programming like AC optimal power flow (OPF) [23-27], research has considered the impact of technical, economic and environmental aspects on the optimal placement of DG.

Although some approaches found in the literature do to some extent consider the inherent time-varying behavior of loads and (renewable) generation patterns[16], [21, 22], [28] there is an absence of methodologies that perform capacity assessments of variable renewable generation based on industry-accepted optimization techniques such as OPF. So here in this thesis the DG capacity assessment of variable renewable generation is based on industry-accepted optimization techniques such as OPF, especially multi-period OPF.

A comparison of decentralized and centralized voltage control on optimal capacity was presented in [29] using a snapshot approach.

In [6], a multi-period AC optimal power flow technique for evaluating network capacity for accommodating variable DG was proposed to offer a means of measuring the impact of ANM (active network management) on connectable renewable capacity, and

consequently increasing the harvesting of energy. In addition to effectively handling the time-variation of multiple renewable sites and demand, it also considers a range of active network techniques to allow maximum absorption of renewable generation capacity while respecting voltage statutory limits and thermal constraints. Active network management control algorithms including coordinated voltage control of transformers and voltage regulators, adaptive power factor control and energy curtailment are embedded within the formulation.

The model used in this thesis for evaluating network capacity for accommodating variable DG is the same model proposed in reference [6] and this thesis has used the first example in reference [6] and the results in this thesis are consistent with those results in reference [6], this thesis does not cover the 2nd example in the research paper in reference [6] as it handles the time-variation of multiple renewable sites and demand while the example in this thesis does not cover multiple renewable sites.

“Network characteristics such as voltage and thermal limits, losses, topology, demand behavior and potential locations for renewable developments, present a number of challenges when formulating the DG capacity allocation problem as a mathematical optimization model. In [23-25], the ability and robustness of using AC OPF to maximize generation capacity and, therefore, identify available headroom was demonstrated, although only using a single, deterministic generation and demand scenario. Extending significantly the work presented in [30], the approach proposed here uses the nonlinear programming (NLP) formulation of a multi-period AC OPF adapted to determine the maximum DG capacity able to be connected to a given network. The objective of maximizing DG capacity (and with it associated energy capture) within the physical limitations of the network and with economically sound levels of curtailment and capacity is entirely credible as the unbundled nature of the distribution business in Europe means that the DNO does not consider energy delivery beyond ensuring that the network can physically handle the power flows with acceptable reliability and cost effectiveness.”[6]

2.3 Minimizing the energy losses and maximizing the difference between the renewable energy and the energy losses

Loss minimization traditionally has focused on network reconfiguration [31, 32], or reactive power support through capacitor placement [33], In general, few studies properly investigate the energy loss minimization problem (as a single or multiple objectives) considering time-varying demand and generation. Here a multi-period AC optimal power flow technique is used to minimize the energy losses by optimally accommodating variable DG and applying some ANM control schemes. Here the same computational frame work originally developed in [6, 30, 34] was employed, the two objective functions of minimization of losses and tradeoff between renewable energy and losses are found in [35], but was applied on the same example in [6]

2.4 The demand side management DSM

A methodology for assessing the potential benefits of using storage and demand side management (DSM) to increase the utilization of network asset is proposed in [36] but the methodology is based on a linear multi-period DC optimal power flow where the DSM and storage are modeled as a part of the optimization constraints. While here in this thesis DSM is modeled also in the optimization constraints in a methodology based on Multi-period AC optimal power flow and using commercial optimization software.

2.5 Summary:

The literature review in this chapter can be summarized as:

Maximizing the DG Capacity:

The literature review can be summarized in four main points:

- “There is an absence of methodologies that perform capacity assessments of variable renewable generation based on industry-accepted optimization technique such as OPF” until the publication of [6]
- The model used in this thesis for evaluating network capacity for accommodating variable DG is the same model proposed in reference [6].
- The study case in this thesis is the first example in reference [6] and the thesis results are consistent with those results in reference [6].
- This thesis uses “Lingo V.13” as an optimization software [37]; while [6] uses “AIMMS” as an optimization software and both software solved the same problems in almost the same time.

Minimizing the energy losses and maximizing the difference between the renewable energy and the energy losses:

The literature review can be summarized in three main points:

- Few studies properly investigated the energy loss minimization problem considering time varying demand and generation until the publication of [35].
- The same multi period AC OPF technique in references [6, 30, 34] and in this thesis was adopted to minimize energy losses in [35].
- The two objective function equations 5-1 and 5-2 are taken from [35] and were applied to the study case in this thesis which is the same study case in [6].

The demand side management:

- Demand side management has been used to increase the DG capacity using a methodology based on linear multi-period DC optimal power flow as in [36].
- In this thesis, a methodology based on multi-period AC optimal power flow and using commercial optimization software is used to increase to the DG capacity and there is an absence of such a methodology in research papers.

.

3

Problem Formulation with Multi-Period AC Optimal Power Flow

Increasing connection of intermittent distributed generation, such as wind power, to distribution networks requires new control strategies to provide greater flexibility and use of existing network assets. Active network management (ANM) will play a major role in this but there is a continuing need to demonstrate the benefit in facilitating connection of new generation without the need for traditional reinforcements. This thesis proposes a multi-period AC optimal power flow (OPF)-based technique for evaluating the maximum capacity of new intermittent distributed generation able to be connected to a distribution network when ANM control strategies are in place. The ANM schemes embedded into the OPF include coordinated voltage control, adaptive power factor, energy curtailment and demand side management. A generic U.K. medium voltage distribution network is analyzed using coincident demand and wind availability data derived from hourly time-series. Results will clearly show that very high penetration levels of new intermittent generation capacity can be achieved by considering ANM strategies compared to the widely used passive operation (i.e., “fit and forget”).

3.1 Mathematical representation of a long distribution cable:

Each distribution cable can be represented by a pi model as shown in the following figure:

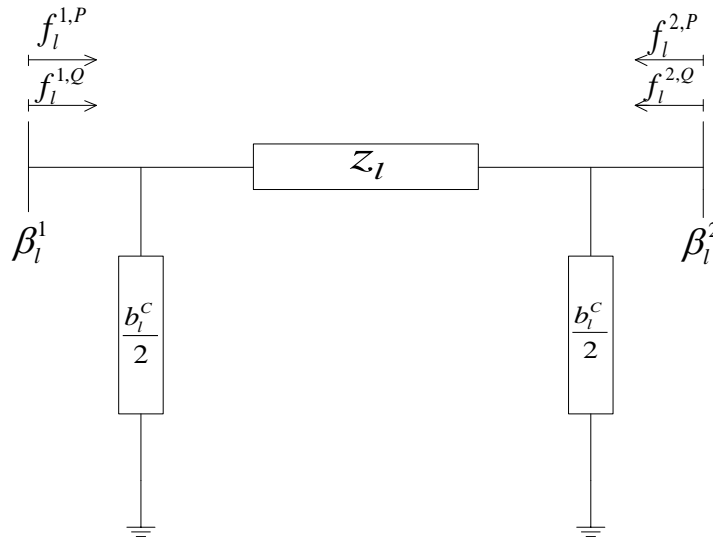


Figure 3-1: Pi Model of a line

And the parameters of the cable can be calculated according to the following equations and with referring to the list of symbols.

$$z_l = r_l + jx_l \quad (3-1)$$

$$y_l = z_l^{-1} = g_l + j.b_l \quad (3-2)$$

$$g_l = \frac{r_l}{r_l^2 + x_l^2} \quad (3-3)$$

$$b_l = -\frac{x_l}{r_l^2 + x_l^2} \quad (3-4)$$

For actual transmission lines and distribution lines the series reactance x_l and the series resistance r_l are both positive, and consequently g_l is positive and b_l is negative. The shunt susceptance b_l^C and shunt conductance g_l^C are both positive for real line sections. In many cases the value of g_l^C is so small that it could be neglected.

3.2 Multi-Period AC OPF model (base case or passive management):

3.2.1 Objective Function:

The Objective of the basic multi-period AC OPF formulation is to maximize the total active DG capacity according to the following objective function:

$$\forall m \in M$$

$$\max \sum_{g \in G} p_g \quad (3-5)$$

3.2.2 Constraints:

The previous objective function is subject to a range of constraints:

- **Voltage at each bus is within an acceptable limit:**

$$V_b^- \leq V_{b,m} \leq V_b^+ \quad (3-6)$$

It is assumed that the voltage magnitude at each bus and during each period m is allowed to change between +6% to -6% of the nominated value, which is one per unit, while in case of passive management, the voltages at the secondary of the OLTC and the secondary voltage of the VR are always fixed and constant, i.e. their secondary voltage magnitude do not change from period to period, thus for passive management cases:

$$V_{b_{OLTC},m} = Constant \quad (3-7)$$

$$V_{b_{VR},m} = Constant \quad (3-8)$$

- **Thermal limit constraint on cables:**

Constraints on the apparent power flow at starting and ending of lines:

$$\forall l \in L \ \& \ \forall m \in M$$

$$(f_{l,m}^{1,P})^2 + (f_{l,m}^{1,Q})^2 \leq (f_l^+)^2 \quad (3-9)$$

$$(f_{l,m}^{2,P})^2 + (f_{l,m}^{2,Q})^2 \leq (f_l^+)^2 \quad (3-10)$$

Where:

β_l^1 : The bus name at the start of the cable.

β_l^2 : The bus name at the end of the cable.

$f_{l,m}^{1,P}$: Active power injection onto line l at the starting bus (β_l^1) and during period m .

$f_{l,m}^{1,Q}$: Reactive power injection onto line l at the starting bus (β_l^1) and during period m .

Equation (3-9) states that the apparent power at the start of line l during period m must be less than a certain thermal limit f_l^+ .

Equation (3-10) states the same but from the end of the cable, at bus (β_l^2).

- **Thermal limit constraint on OLTC and VR:**

For an on load tap changer OLTC or a voltage regulator, each is considered as a single line with the active power at the sending bus and during each period m is $f_{l,m}^{1,P}$ and the reactive power at the receiving end bus and during each period m is $f_{l,m}^{1,Q}$, and equation (3-9) also applies, stating that the apparent power passing through an OLTC or a VR is limited.

Also the same thermal limit constraint of the OLTC and the VR is taken into consideration if the apparent power flow is in the opposite direction by substituting with equations (3-13) and (3-14) into equation (3-10).

$$f_{l,m}^{1,P} = g_l \cdot V_{\beta_l^1}^2 - V_{\beta_l^1} \cdot V_{\beta_l^2} \cdot [g_l \cdot \cos(\delta_{\beta_l^1} - \delta_{\beta_l^2}) + b_l \cdot \sin(\delta_{\beta_l^1} - \delta_{\beta_l^2})] \quad (3-11)$$

$$f_{l,m}^{1,Q} = -b_l \cdot V_{\beta_l^1}^2 - V_{\beta_l^1} \cdot V_{\beta_l^2} \cdot [g_l \cdot \sin(\delta_{\beta_l^1} - \delta_{\beta_l^2}) - b_l \cdot \cos(\delta_{\beta_l^1} - \delta_{\beta_l^2})] \quad (3-12)$$

$$f_{l,m}^{2,P} = g_l \cdot V_{\beta_l^2}^2 - V_{\beta_l^2} \cdot V_{\beta_l^1} \cdot [g_l \cdot \cos(\delta_{\beta_l^2} - \delta_{\beta_l^1}) + b_l \cdot \sin(\delta_{\beta_l^2} - \delta_{\beta_l^1})] \quad (3-13)$$

$$f_{l,m}^{2,Q} = -b_l \cdot V_{\beta_l^2}^2 - V_{\beta_l^2} \cdot V_{\beta_l^1} \cdot [g_l \cdot \sin(\delta_{\beta_l^2} - \delta_{\beta_l^1}) - b_l \cdot \cos(\delta_{\beta_l^2} - \delta_{\beta_l^1})] \quad (3-14)$$

A mathematical proof of equations (3-11), (3-12), (3-13) and (3-14), and is driven in the appendices A.2:”Proof of power flow equations”

When tap changers capabilities exist in l (e.g., OLTCs, VRs), the corresponding terms for the voltage at the start bus of the line, i.e., $V_{B_{l,m}}^1$ must be divided by $T_{OLTC,m}$ or $T_{VR,m}$, where:

$$T_{OLTC,m} = Constant \quad (3-15)$$

$$T_{VR,m} = Constant \quad (3-16)$$

For passive networks, voltage control is usually based on a simple constant voltage policy or a scheme that takes into account circuit loading while determining the voltage that should be maintained. It is important to mention that this voltage control policy was designed for passive networks with strictly unidirectional power flows, so in a traditional (passive) networks, substation secondary voltages (secondary of the OLTC) and the secondary of the voltage regulator have fixed voltage values which don't change with the periods at a corresponding fixed tap position, so the tap position for the OLTC and the tap position for the voltage regulator is always fixed.

It is important to mention that optimization problems are classified from the most easiest to the most difficult as in Table A-1 in Appendix according to the help of the software used in the thesis [37], the optimization problem is a non-linear optimization problem, so the tapping of the OLTC and that of the VR will have a continuous real value and it is not a discrete value, so the model is a NLP “non-linear problem” otherwise if the tapping positions of the OLTC and the VR were to have discrete values to resemble the actual and exact situation, the model becomes an mixed integer nonlinear problem and it will be much harder to solve according to the table in the Appendix. In the later study case in this chapter the implemented the model is a non-linear model. This nonlinear model will solve within 30 seconds to 40 minutes depending on each case, while implementing a mixed integer nonlinear model will solve for some of the cases in around 30 hours while for other cases, there is no solution. It has been found that when using the mixed integer nonlinear model, the maximum DG capacity is almost the same as that given by the use of the non-linear model but with an error around +/- 1%.

The only advantage of the mixed integer non-linear model is that it gives discrete values in the solution regarding the tapping of the OLTC and the VR.

Then continuing with other constraints, the Kirchhoff's current law describing the active and reactive power balance at each node bus, so:

- **Active and reactive power balance at each node bus :**

This case will be referred to it by the “NO curtailment” and it means the active and reactive power balance equations at each node bus without energy curtailment, and the energy curtailment will be explained later in this chapter.

The active power balance at each node bus is:

$$\begin{aligned}
 \sum_{l \in L \& \beta_l^1 = b} f_{l,m}^{1,P} + \sum_{l \in L \& \beta_l^2 = b} f_{l,m}^{2,P} + d_b^P \eta_m \\
 = \sum_{g \in G \& \beta_g = b} p_g w_m + \sum_{x \in X \& \beta_x = b} p_{x,m}
 \end{aligned} \tag{3-17}$$

The reactive power balance equation at each node bus and in the case of capacitive power factor is:

$$\begin{aligned}
 \sum_{l \in L \& \beta_l^1 = b} f_{l,m}^{1,Q} + \sum_{l \in L \& \beta_l^2 = b} f_{l,m}^{2,Q} + d_b^Q \eta_m \\
 - \frac{(V_{b,m})^2}{2} \left[\sum_{l \in L \& \beta_l^1 = b} b_l^c + \sum_{l \in L \& \beta_l^2 = b} b_l^c \right] \\
 = \sum_{g \in G \& \beta_g = b} p_g w_m \tan(\phi_{g,m}) + \sum_{x \in X \& \beta_x = b} q_{x,m}
 \end{aligned} \tag{3-18}$$

While the reactive power balance equation at each node bus and in the case of inductive power factor is:

$$\begin{aligned}
 \sum_{l \in L \& \beta_l^1 = b} f_{l,m}^{1,Q} + \sum_{l \in L \& \beta_l^2 = b} f_{l,m}^{2,Q} + d_b^Q \eta_m \\
 - \frac{(V_{b,m})^2}{2} \left[\sum_{l \in L \& \beta_l^1 = b} b_l^c + \sum_{l \in L \& \beta_l^2 = b} b_l^c \right] \\
 = - \sum_{g \in G \& \beta_g = b} p_g w_m \tan(\phi_{g,m}) + \sum_{x \in X \& \beta_x = b} q_{x,m}
 \end{aligned} \tag{3-19}$$

- **Power factor constraint at the DG bus:**

In passive networks the DNO's operate the DG units at constant power factors over all load conditions and during each period and the following constraint applies:

$$PF_{g,m} = \text{constant} \tag{3-20}$$

$$PF_{g,m} = \cos(\phi_{g,m}) \tag{3-21}$$

$$\phi_{g,m} = \text{constant} \tag{3-22}$$

In passive distribution networks, the least cost effective solution for a wind farm is the operation at constant power factor close to unity of each individual wind turbine generator and this is this is the classical approach for small wind farms (only a few turbines) connected to distribution grids ($\leq 33\text{kV}$). But the fixed values of the fixed power factor may be changed occasionally, for example for winter and summer, or peak and no-load periods, the power factor values taken in this thesis are 1, 0.98 lagging and 0.98 leading.

- **Other constraints:**

The distribution network has external connections at the grid supply points (GSP) substation as well as interconnectors. Both can export power so the import/export constraints at the interconnector x are:

$$\forall x \in X \ \& \ \forall m \in M$$

$$p_x^- \leq p_{x,m} \leq p_x^+ \quad (3-23)$$

$$q_x^- \leq q_{x,m} \leq q_x^+ \quad (3-24)$$

The GSP is taken as the reference (slack) bus b_o with the voltage angle set at zero so:

$$\forall m \in M$$

$$\delta_{b_o,m} = 0 \quad (3-25)$$

3.3 Incorporating Active Network Management

With ANM, DNOs will be capable of optimizing use of their assets by dispatching generation, Controlling OLTC (On Load Tap Changers) and voltage regulators, managing reactive power, and reconfiguring the system [4, 11, 38].

Implementation of such schemes will require complex control techniques, while the actual actuation of devices (e.g., tap changers) will depend on their respective response time-scales. As the proposed technique is designed for use at the planning stage, it is assumed that network components respond immediately to control actions, and have effectively one (steady) state in each period (m)[6].

3.3.1 Coordinated Voltage Control

The desired voltages at the node buses can be kept within acceptable limits by either directly controlling the voltage or by controlling the reactive power flow. The equipment normally used for the voltage and reactive power control are on-load tap-changer (OLTC) transformers, switched shunt capacitors and steps voltage regulator [39, 40]

An on-load tap changer transformer (OLTC), is a transformer with automatically adjustable taps, typically with steps of 1-3 %. And discrete valued control, capable of regulating the voltage of the secondary side of a transformer at one point in the network, is usually available in the distribution system for this purpose. While a step voltage regulator is an autotransformer with automatically adjustable taps, which is usually installed when the feeder is too long especially when voltage regulation with OLTC and shunt capacitors is not sufficient to keep the voltage within acceptable limits. Voltage and reactive power control involves proper coordination among the available voltage and reactive power control equipment.

So why is there a need for a voltage regulator? Isn't the presence of the OLTC sufficient? The main use of OLTC transformer is to reduce the voltage on the feeder where the DG is connected, but this might produce unacceptable voltage drops on adjacent feeders that supply the load. In this case, it may be beneficial to separate the control of voltage on feeders that supply load from the control of voltage on feeders to which the DG is connected. This can be achieved by the application of voltage regulators.

The use of coordinated voltage control with on-load tap changers enables the connection of an increased DG capacity by actively changing the OLTC transformer setting and maintaining the voltages of a distribution network within defined limits.

The word coordination comes from choosing the proper tap setting of both the OLTC and the voltage regulator during each period.

For a complex network configuration, the OLTC transformer and voltage regulator tap settings can be determined by optimization techniques but as mentioned before, for simplicity, the taps will have continuous values and not discrete values to avoid changing the model from non-linear model to a mixed non-linear model which has much higher complexity.

Instead of having the voltage control based on a simple constant voltage policy as in passive network, in active management, coordinated voltage control is applied by dynamically controlling the OLTC at the substation and the corresponding distribution secondary voltage, and thus more DG capacity can be connected without triggering reinforcement costs [4, 6]. Thus, in each period the secondary voltage of the OLTC will be treated as a variable, rather than a fixed parameter, while maintaining its value within the statutory range; $\forall m \in M$:

$$V_{b_{OLTC}}^- \leq V_{b_{OLTC},m} \leq V_{b_{OLTC}}^+ \quad (3-26)$$

$$V_{b_{V.R}}^- \leq V_{b_{V.R},m} \leq V_{b_{V.R}}^+ \quad (3-27)$$

$$t_{OLTC}^- \leq T_{OLTC,m} \leq t_{OLTC}^+ \quad (3-28)$$

$$t_{VR}^- \leq T_{VR,m} \leq t_{VR}^+ \quad (3-29)$$

The tapings of the OLTC and the VR are optimized to certain continuous values between limits according to equations (3-28) and (3-29).

3.3.2 Adaptive Power Factor Control (PFc) or Coordinated Generator Reactive Power Control

Wind turbines especially those equipped with power electronic controllers should be able to provide necessary reactive power support to the grid and this reactive power needed could be centrally dispatched by Distribution Network Operators (DNO's), in other words the power factor of the wind turbines could be controlled so that the wind energy penetration level is maximized. The proposed control scheme requires wind turbines to

generate reactive power during load peak hours and low generation and to absorb reactive power during load off-peak hours and high generation [6, 41]. So in practice DG will be required to operate within a certain range of power factor.

In the recent grid codes of many countries such as Denmark, Germany, Italy, Ireland and the UK, it is required that the wind turbines provide reactive power control capabilities and that network operators may specify power factor or reactive power generation requirement for grid-connected wind turbines.

In practice, a grid connected wind turbine needs to fulfill the specific requirements depending on the regulation of the country. For example according to [41]:

- In the Danish grid code for grid connected wind turbines, reactive power generation is confined to a control band with respect to active power generation (with a power factor between 1.00 and 0.925 lagging).
- The German code specifies different reactive power limits according to voltage value at the interconnection (with a power factor ranging between 1.00 and 0.925 lagging).
- The Irish grid code requires a power factor between 0.835 leading and 0.835 lagging when the active power level is below 50% of the rated capacity.
- In Italy and the UK, the power factor at Wind Turbine's terminal should be between 0.95 leading and 0.95 lagging.

Although it is important to fulfill the grid code when connecting a wind turbine, this thesis intends to illustrate the concept of the proposed method without designing a wind turbine that fulfills a specific requirement.

So to conclude that in practice the DG will be required to operate within a certain range of power factor PF_g^+ -, the following constraint applies:

$$PF_g^- \leq PF_{g,m} \leq PF_g^+ \quad (3-30)$$

$$PF_{g,m} = \cos(\phi_{g,m}) \quad (3-31)$$

$$\phi_g^- \leq \phi_{g,m} \leq \phi_g^+ \quad (3-32)$$

3.3.3 Energy Curtailment

The main idea behind the generation curtailment is that a power producer may find it economically convenient to be cut off in some circumstances if the power producer can install bigger power generator and sell energy most of the time [42].

This active power generation curtailment is a type of control that may be effective when the generator is connected to a weak network, with a high R/X ratio. It is profitable to curtail some of the active power output of the wind generator for a limited period to allow connection of larger capacity and to avoid network reinforcement. Generation wind curtailment is likely to be required during times when minimum demand coincides with high output, such as summer nights in Sweden.

The active power generation curtailment is a local voltage control scheme, which controls the voltage by constraining the active power of the DG to limit the voltage rise, and it is very useful because it allows a larger plant capacity to be connected

So in order to alleviate the over-voltage problem and the thermal network limits which restrict the DG capacity specially at minimum demand , it may be necessary to curtail a certain amount of wind energy injected into the network [4]. Although the wind energy output is reduced, The Wind Turbine developer may still gain more profits due to the possibility of installing more wind turbines [43].

In the proposed method the wind energy may be curtailed during certain periods in order to alleviate any voltage or thermal constraint violation. For example, for a specific period, there are different possible combinations of load demand and wind power. Wind energy is curtailed at the combination of minimum demand and maximum wind power.

Power curtailment is formulated here by adding a negative generation (or positive demand) variable ($p_{g,m}^{curt}$) at the same location of each DG unit, solely affecting the constraints related to active and reactive nodal power balance. Thus equations (3-17), (3-18) and (3-19) are adapted by adding the terms $\sum_{g \in G_b} p_{g,m}^{curt}$ and $\sum_{g \in G_b} p_{g,m}^{curt} \tan(\phi_{g,m})$, respectively, thus the active power balance equation becomes:

$$\begin{aligned} \sum_{l \in L \& \beta_l^1 = b} f_{l,m}^{1,P} + \sum_{l \in L \& \beta_l^2 = b} f_{l,m}^{2,P} + d_b^P \eta_m \\ = \sum_{g \in G_b \& \beta_g = b} p_g w_m - \sum_{g \in G_b} p_{g,m}^{curt} + \sum_{x \in X \& \beta_x = b} p_{x,m} \end{aligned} \quad (3-33)$$

And the reactive power balance equation in case of capacitive power factor:

$$\begin{aligned} \sum_{l \in L \& \beta_l^1 = b} f_{l,m}^{1,Q} + \sum_{l \in L \& \beta_l^2 = b} f_{l,m}^{2,Q} + d_b^Q \eta_m \\ = \sum_{g \in G_b \& \beta_g = b} p_g w_m \tan(\phi_{g,m}) - \sum_{g \in G_b} p_{g,m}^{curt} \tan(\phi_{g,m}) \\ + \sum_{x \in X \& \beta_x = b} q_{x,m} - \frac{(V_b)^2}{2} \left[\sum_{l \in L \& \beta_l^1 = b} b_l^c + \sum_{l \in L \& \beta_l^2 = b} b_l^c \right] \end{aligned} \quad (3-34)$$

While the reactive power balance equation for the case of inductive power factor:

$$\begin{aligned}
 & \sum_{l \in L \& \beta_l^1 = b} f_{l,m}^{1,Q} + \sum_{l \in L \& \beta_l^2 = b} f_{l,m}^{2,Q} + d_b^Q \eta_m - \frac{(V_b)^2}{2} \left[\sum_{l \in L \& \beta_l^1 = b} b_l^c + \sum_{l \in L \& \beta_l^2 = b} b_l^c \right] \\
 & = - \left[\sum_{g \in G_b \& \beta_g = b} p_g w_m \tan(\phi_{g,m}) - \sum_{g \in G_b} p_{g,m}^{curt} \tan(\phi_{g,m}) \right] \quad (3-35) \\
 & + \sum_{x \in X \& \beta_x = b} q_{x,m}
 \end{aligned}$$

To examine the impact of different allowed levels of curtailment on overall DG capacity, the total amount of curtailed energy from each DG will be restricted to a curtailment factor λ_{curt} , a percentage of the potential energy that could have otherwise been delivered by each DG. The following constraint follows:

$$\begin{aligned}
 & \forall g \in G : \\
 & \sum_{m \in M} p_{g,m}^{curt} \cdot \tau_m \leq \lambda_{curt} \left[\sum_{m \in M} p_g w_m \tau_m \right] \quad (3-36)
 \end{aligned}$$

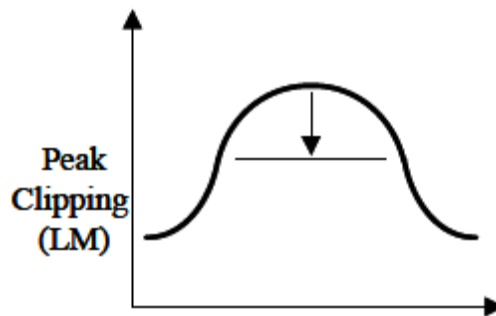
The curtailment variables $p_{g,m}^{curt}$ need to be limited to the output of g at the corresponding period:

$$\begin{aligned}
 & \forall g \in G : \\
 & p_{g,m}^{curt} \leq p_g w_m \quad (3-37)
 \end{aligned}$$

3.3.4 Demand Side Management DSM:

Demand-side management (DSM) has been traditionally seen as a means of reducing peak electricity demand; Loads are externally controlled for the set of DSM actions when the end-users are provided with the needed hardware and communication infrastructure to allow direct load control. The customers' load is interrupted by remotely shutting down or cycling consumers' electrical appliances such as air conditioners and water heaters.

Reducing peak electricity demand can be down as shown (also known as Peak clipping)



Usually, the goal of demand side management is to encourage the consumer to use less energy during peak hours

DSM is one kind of the ANM and can be used as a method to increase the DG capacity and increase the renewable energy penetration from the DG as will be shown with coming model.

Let the objective function to be maximizing the connected DG capacity:

$$\forall m \in M$$

$$\max \sum_{g \in G} P_G \quad (3-38)$$

Subject to all the constraints from Equation in the base model except the constraints regarding the active and reactive power balance at each node bus which need to be modified.

The active power balance at each node bus is:

$$\sum_{l \in L \ \& \ \beta_l^1 = b} f_{l,m}^{1,P} + \sum_{l \in L \ \& \ \beta_l^2 = b} f_{l,m}^{2,P} + d_b^P \cdot \eta_m - dP_{b,m}^{Curtail}$$

$$= \sum_{g \in G_b \ \& \ \beta_g = b} p_g w_m + \sum_{x \in X \ \& \ \beta_x = b} p_{x,m} \quad (3-39)$$

Where the active power demand curtailed at bus b during period m is $dP_{b,m}^{curtail}$ and is limited according to the following:

$$d_{b,m}^{Curtail} \leq f_{b,m} * d_b^P \eta_m \quad (3-40)$$

$$f^{min} \leq f_{b,m} \leq f^{max} \quad (3-41)$$

In our study case:

$$f^{min} = 0 \quad (3-42)$$

$$f^{max} = 0.02, OR, f^{max} = 0.05, OR, f^{max} = 0.1, OR, f^{max} = 0.2 \quad (3-43)$$

Hint: f^{max} does not have a unit.

The active power demand curtailed at bus b during period m is $dP_{b,m}^{curtail}$ and the reactive power demand curtailed at bus b during period m is $dQ_{b,m}^{curtail}$ and both are related to each other by the derived equation (3-47).

$$dP_{b,m} = d_b^P \cdot \eta_m \quad (3-44)$$

$$dQ_{b,m} = d_b^Q \cdot \eta_m \quad (3-45)$$

$$\frac{dQ_{b,m}}{dP_{b,m}} = \frac{d_b^Q}{d_b^P} \quad (3-46)$$

$$dQ_{b,m}^{curtail} = dP_{b,m}^{curtail} * \left(\frac{d_b^Q}{d_b^P}\right) \quad (3-47)$$

The reactive power balance equation at each node bus and in the case of capacitive power factor is:

$$\begin{aligned} & \sum_{l \in L \& \beta_l^1 = b} f_{l,m}^{1,Q} + \sum_{l \in L \& \beta_l^2 = b} f_{l,m}^{2,Q} + d_b^Q \eta_m - dQ_{b,m}^{curtail} \\ & - \frac{(V_{b,m})^2}{2} \left[\sum_{l \in L \& \beta_l^1 = b} b_l^c + \sum_{l \in L \& \beta_l^2 = b} b_l^c \right] \\ & = \sum_{g \in G \& \beta_g = b} p_g w_m \tan(\phi_{g,m}) + \sum_{x \in X \& \beta_x = b} q_{x,m} \end{aligned} \quad (3-48)$$

While the reactive power balance equation at each node bus and in the case of inductive power factor is:

$$\begin{aligned} & \sum_{l \in L \& \beta_l^1 = b} f_{l,m}^{1,Q} + \sum_{l \in L \& \beta_l^2 = b} f_{l,m}^{2,Q} + d_b^Q \eta_m - dQ_{b,m}^{curtail} \\ & - \frac{(V_{b,m})^2}{2} \left[\sum_{l \in L \& \beta_l^1 = b} b_l^c + \sum_{l \in L \& \beta_l^2 = b} b_l^c \right] \\ & = - \sum_{g \in G \& \beta_g = b} p_g w_m \tan(\phi_{g,m}) + \sum_{x \in X \& \beta_x = b} q_{x,m} \end{aligned} \quad (3-49)$$

4

Case Study, Simplified EHV1 Network-Single DG

In this chapter, different active management schemes are applied to a simplified EHV1 Network from the U.K. Generic Distribution System in order to maximize the DG capacity of a connected wind farm using the multi period AC optimal power flow, the demand side management (DSM) active management scheme will be applied to the same generic distribution system and the results will be analyzed separately at the end of the same chapter.

4.1 Study Case

4.1.1 Data and assumptions

A sample of the hourly demand for central Scotland in 2003 is shown in Figure 4-1 along with coincident wind production of two different wind sites (named here, WP1 and WP2). The wind production data were derived from U.K. Meteorological Office measured wind speed data and have been processed and applied to a generic wind power curve [44].

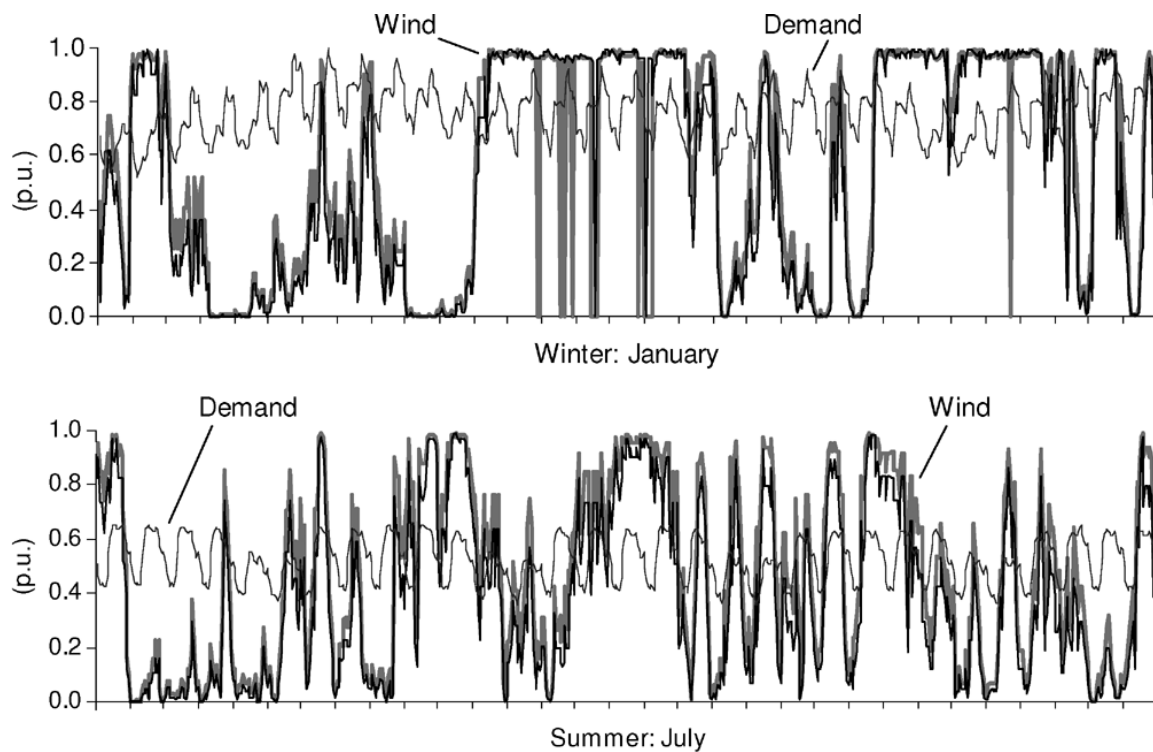


Figure 4-1: (Top) Winter and (bottom) Summer hourly demand and wind power production (relative to peak) for central Scotland, 2003[44]. Two different wind profiles are considered: WP1(black line) and WP2(grey line).

One way to reduce the computational burden of a full time-series analysis is to aggregate wind availability and demand into a manageable number of wind/demand scenarios based on their joint probability of occurrence[6]. The “duration” of each scenario is then the number of coincident hours which it represents. Only 74 non-zero scenarios are effectively considered in the analysis [6] and more details are in [6].

4.1.2 Load data and wind power data:

Table 4-1: Coincident hours for each of the demand/generation scenarios [6].

10	103	158	192	127	53	2	0%	% of Generation Capacity
43	303	451	515	339	156	11	10%	
20	136	226	336	175	73	15	20%	
16	147	201	276	138	45	6	30%	
11	79	170	212	113	41	4	40%	
7	63	130	161	84	33	7	50%	
0	60	147	172	85	41	4	60%	
1	40	132	143	95	33	4	70%	
0	48	123	176	90	42	8	80%	
2	54	144	212	110	48	6	90%	
0	63	257	559	305	152	16	100%	
40%	50%	60%	70%	80%	90%	100%		
% of Peak Demand								

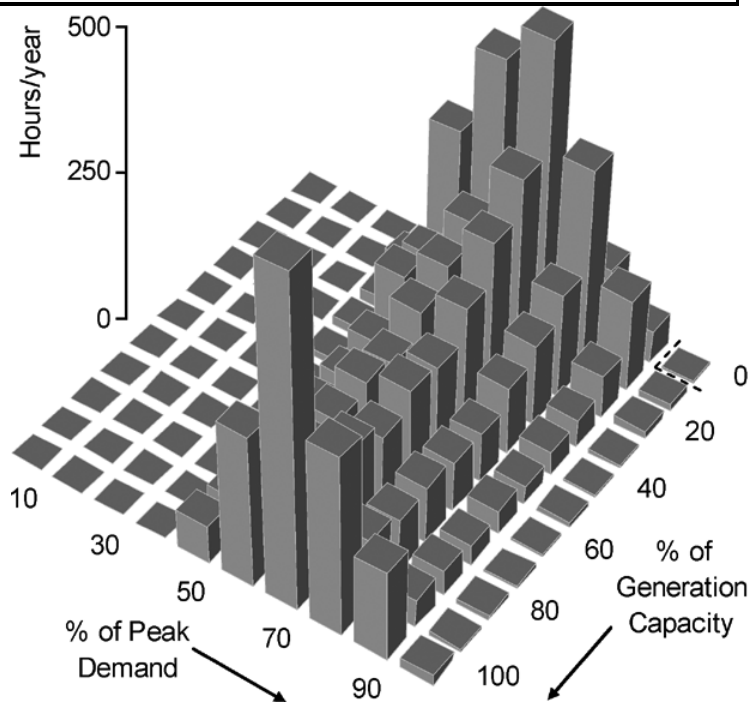


Figure 4-2: coincident hours for each of the demand/generation scenarios [6].

The summation of the total period hours is 8760 hours, corresponding to one year.

4.1.3 Network Data

Figure 4-3 shows the Simplified EHV1 Network from the U.K. Generic Distribution System (GDS). Full data for this 16-bus 33-kV rural weakly meshed network are available in [45] and all the necessary data needed for this study case has also been revised and summarized in the appendices. The feeders are supplied by two identical 30-MVA 132/33-kV transformers. The GSP voltage is assumed to be nominal. In the demand-only case (no DG), the OLTC at the substation has a target voltage of 1.036 p.u. at the secondary. A voltage regulator (VR) is located between buses 8 and 9, with the latter having a target voltage of 1.03 p.u. Voltage limits are 6% of nominal, reflecting U.K. practice. A single DG unit is located at bus 16 driven by the aggregated wind profile WP1. The total peak demand is 38.2 MW.

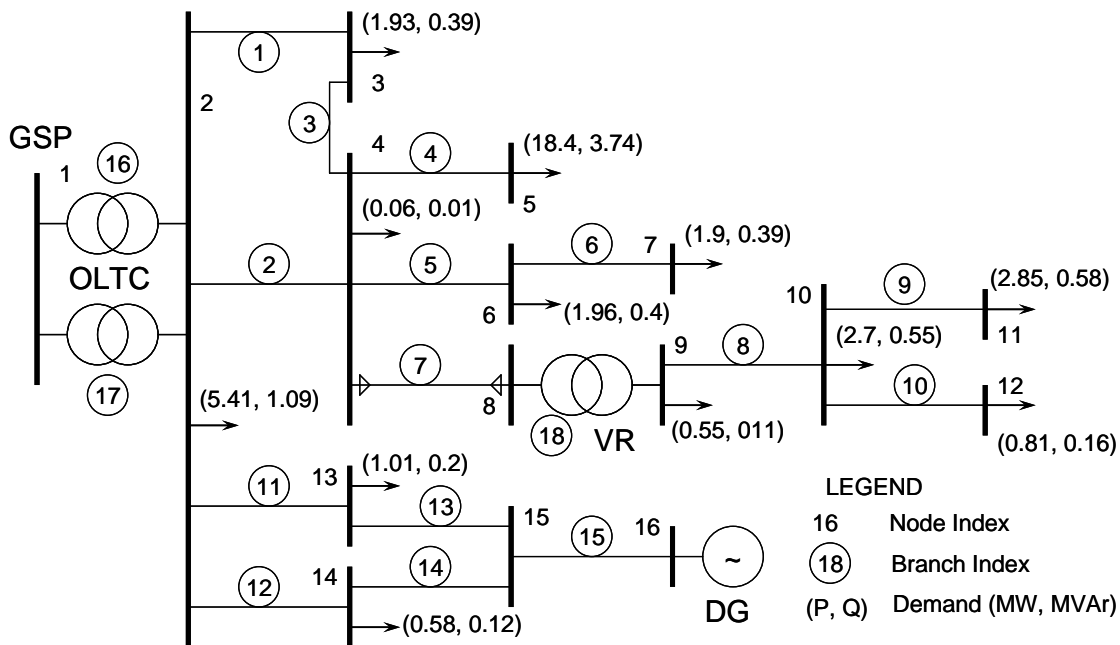


Figure 4-3:U.K. GDS simplified EHV1 network at maximum load [6].

The demand/wind scenarios from [44] along with a range of passive and progressively more active network management schemes were applied to the network. The maximum wind power capacity that can be accommodated at node 16 was investigated considering: the coordinated voltage control (CVC) of the OLTC and the voltage regulator; adaptive power factor control (PFc); and different maximum levels of curtailment. This will result in 20 different cases to consider for studying as in Table 4-2.

Table 4-2: The 20 different scenarios/cases, where cases A, B and C represent passive operation and the other cases are active management cases.

Case	Passive	Active
------	---------	--------

	A	B	C	D	E	F	G	H	I	J	K	L	M	N	O	P	Q	R	S	T
PF=0.98 capacitive	✓				✓				✓				✓				✓			
Pf=1 Unity		✓				✓				✓				✓				✓		
PF=0.98 inductive			✓				✓				✓				✓				✓	
$0.95 \leq PF \leq 0.98$ inductive				✓				✓				✓				✓				✓
No CVC + No Curtailment	✓	✓	✓	✓																
CVC + No Curtailment					✓	✓	✓	✓												
CVC + 2% Curtailment									✓	✓	✓	✓								
CVC + 5% Curtailment													✓	✓	✓	✓				
CVC + 10% Curtailment																	✓	✓	✓	✓

For full understanding on how to build the model and implementation of the above equations, the general equations described early in this chapter were applied to each bus and to each line in our case study of the UK network, thus allowing better understanding even with implementation of other software's than the one used in this thesis. See "A.5: Implementation" in the Appendices.

The optimization software used is called Lingo [37] and is a product of Lindosystems , It is worth mentioning that each case is a huge non-linear problem with around 8000 variables and there is no guarantee that the solution is the global solution, but each case in this thesis was solved with a nonlinear optimality tolerance of 1e-007 and a final nonlinear feasibility tolerance of 1e-006. The "Multi Start" option was applied in each case to ensure that the solution is not a local optimum point, but in order to get a global solution, the "Global Solver" has to be invoked, which results that each case will take a couple of days to solve.

4.2 Results and Analysis of the Study Case:

With the objective of maximizing the DG capacity, the results are shown in Figure 4-4. It is clear from Figure 4-4 that only three active management schemes are implemented which are:

- 1- Adaptive Power Factor Control (PFc)

- 2- Coordinated Voltage Control (CVC)
- 3- Energy Curtailment

While the demand side management control scheme DSM will be treated alone at the end of this chapter.

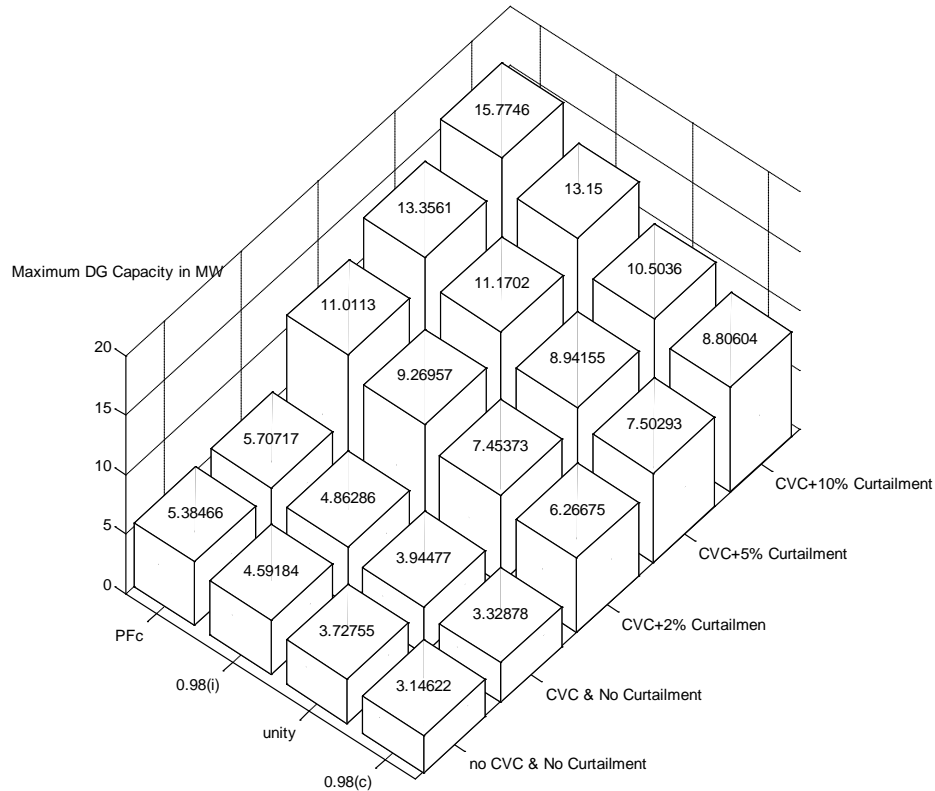


Figure 4-4: Simplified EHV1 network: connectable DG capacity (in MW) with ANM strategies (capacitive, i: inductive, and PFc: adaptive power factor control).

According to Figure 4-4, a table of the different 20 cases and their maximum DG capacity is shown in Table 4-3.

Table 4-3: The 20 different cases and their maximum DG capacity.

Case	Power Factor	CVC	Energy Curtailment	Maximum DG Capacity
A	0.98 (c)	NO	NO	3.14622
B	1	NO	NO	3.72755
C	0.98 (i)	NO	NO	4.59184
D	PFcontrol	NO	NO	5.38466
E	0.98 (c)	NO	NO	3.32878
F	1	NO	NO	3.94477
G	0.98 (i)	NO	NO	4.86286
H	PFcontrol	NO	NO	5.70717
I	0.98 (c)	YES	YES (2%)	6.26675
J	1	YES	YES (2%)	7.45373

K	0.98 (i)	YES	YES (2%)	9.26957
L	PFcontrol	YES	YES (2%)	11.0113
M	0.98 (c)	YES	YES (5%)	7.50293
N	1	YES	YES (5%)	8.94155
O	0.98 (i)	YES	YES (5%)	11.1702
P	PFcontrol	YES	YES (5%)	13.3561
Q	0.98 (c)	YES	YES (10%)	8.80604
R	1	YES	YES (10%)	10.5036
S	0.98 (i)	YES	YES (10%)	13.15
T	PFcontrol	YES	YES (10%)	15.7746

4.2.1 Comparison between two study cases using graphs

A comparison between case D and case T will be done, where according to Table 4-3:

- Case D: has inductive power factor between 0.95 and 0.98 inductive (has power factor control only) and thus without coordinated voltage control CVC and without energy Curtailment, but case D is still considered an active management case but with one control scheme (Power factor control).
- Case T: has inductive power factor between 0.95 and 0.98 and coordinated voltage control CVC and 10% energy curtailment, and is an active management case with three different active management control schemes.

The accuracy of the results in Figure 4-4 were found to be the same as those in [6], using graphs the difference between case D and case T will be shown by comparing in both cases:

- The secondary voltage of the OLTC ($V_{2_{OLTC,m}}$).
- The secondary voltage of VR ($V_{9_{VR,m}}$).
- Tapping position of OLTC ($T_{OLTC,m}$).
- Tapping position in VR ($T_{VR,m}$).
- The voltage magnitude at the most far bus from sources ($V_{12,m}$),
- External reactive power support needed.
- Active power curtailed.
- Active power from the DG
- Active power from the Slack Bus.

Comparison based on the secondary voltages and tapping position

For case D, according to Figure 4-5, the tapping of both the OLTC and the VR are constant during all the periods and do not change from period to another, the value of the tapping is the “starting tap ratio” TTR which has a value of 0.97 and 0.92 respectively according to Table A- 5 in the Appendices. The secondary voltage for the OLTC and the VR has fixed values of 1.036 pu and 1.03 respectively and these values are the “target voltage magnitudes” found in Table A- 2 in the Appendices and these voltage magnitudes are fixed for all the periods and do not change from period to period. The reason for having fixed tapping values with the periods and fixed secondary voltage with the periods

is that the case D does not have coordinated voltage control scheme. Thus, the same applies for cases A, B, C in Table 4-3.

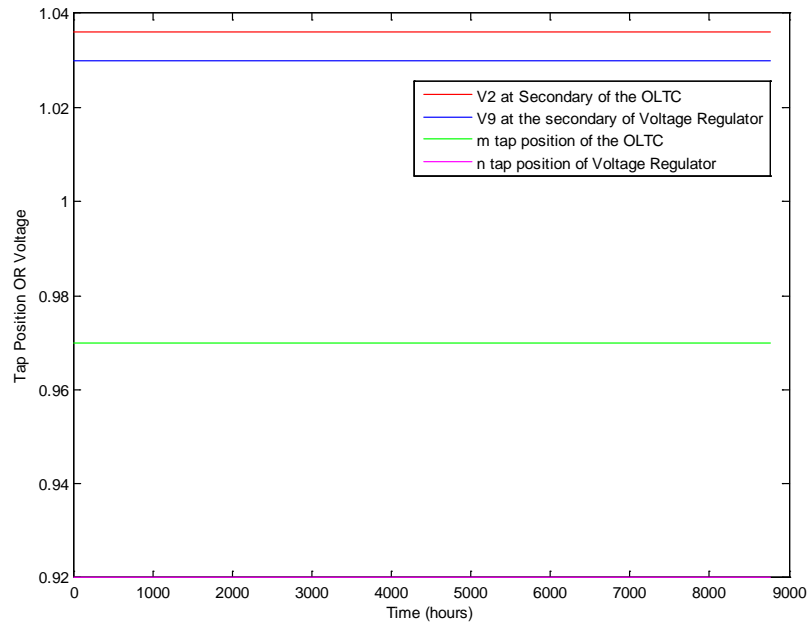


Figure 4-5: Tapping position for OLTC and VR together with the secondary voltage of both OLTC and VR for case D

On the other hand, for case T and according to Figure 4-6, the tapping of both the OLTC and the VR change instantly from period to another and are limited between 1.05 (the maximum tap position) and 0.85 (the minimum tap position) found in Table A- 5 in the Appendices and in accordance with equation (3-28) and equation (3-29). The secondary voltage of the OLTC and that of the VR change instantly from period to another between the maximum voltage limit of 1.06 pu and the minimum voltage limit of 0.94 pu found in Table A- 2 in the Appendices and according to equation (3-26) and equation (3-27). The reason for having variable tapping values with the periods and variable secondary voltage with the periods is that case T has coordinated voltage control (CVC) scheme. Thus, the same applies for cases E, F, G, H, I, J, K, L, M, N, O, P, Q, R and S in Table 4-3.

It is important to mention that in order to get the Figure 4-5, Figure 4-6 and Figure 4-7, and all the graphs in this comparison between case T and case D, the periods were taken from Table 4-1, starting with the period of 10 hours and then 103 hours and ending up with period of 16 hours, were the summation of the total period hours is 8760 hours, corresponding to one year, and hence each period with the corresponding voltage or tapping in that period was drawn using Matlab.

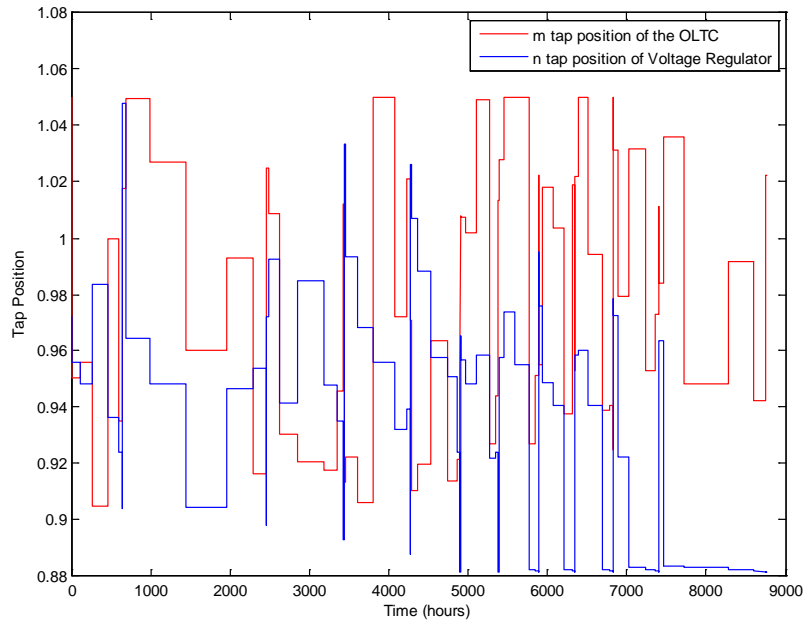


Figure 4-6: Tapping position of the OLTC & VR for case T

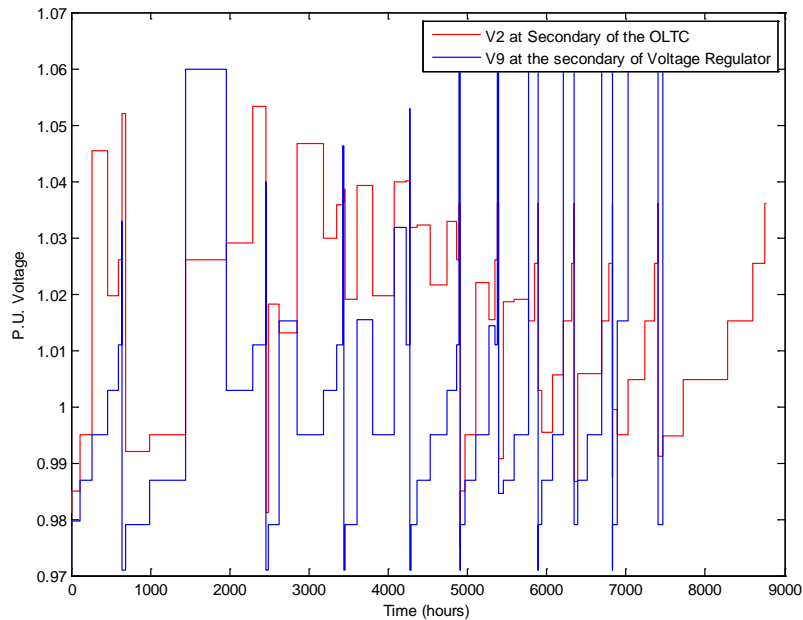


Figure 4-7: Secondary voltage of OLTC & VR for case T

Comparison based on voltage magnitude at bus 12:

Bus 12 is the most far bus from both the two available sources, it has been found that for both cases D and T, the voltage value during each period is within acceptable limits and between minimum voltage of 0.94 pu and maximum voltage of 1.06 pu and this is obvious since equation (3-6) is applicable for all the 20 different cases.

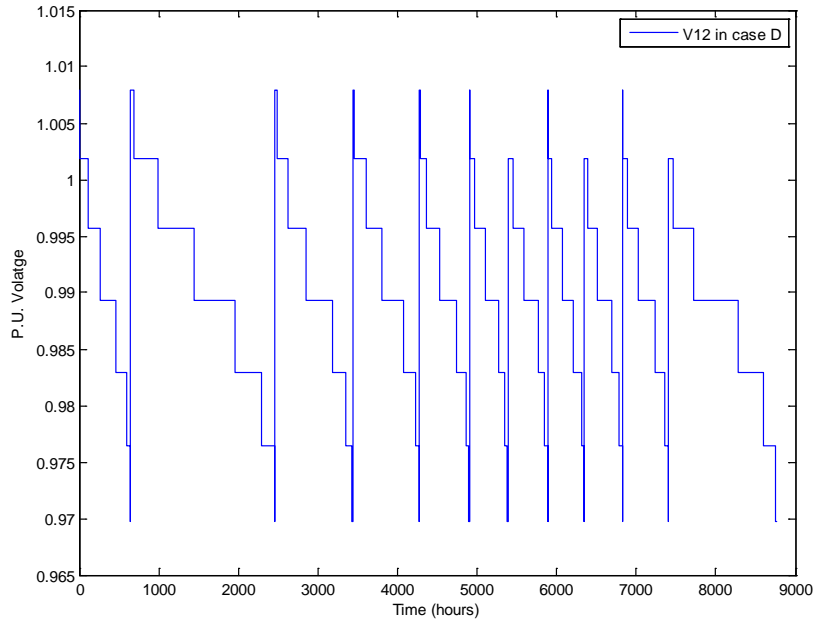


Figure 4-8: Voltage magnitude at bus 12 for case D.

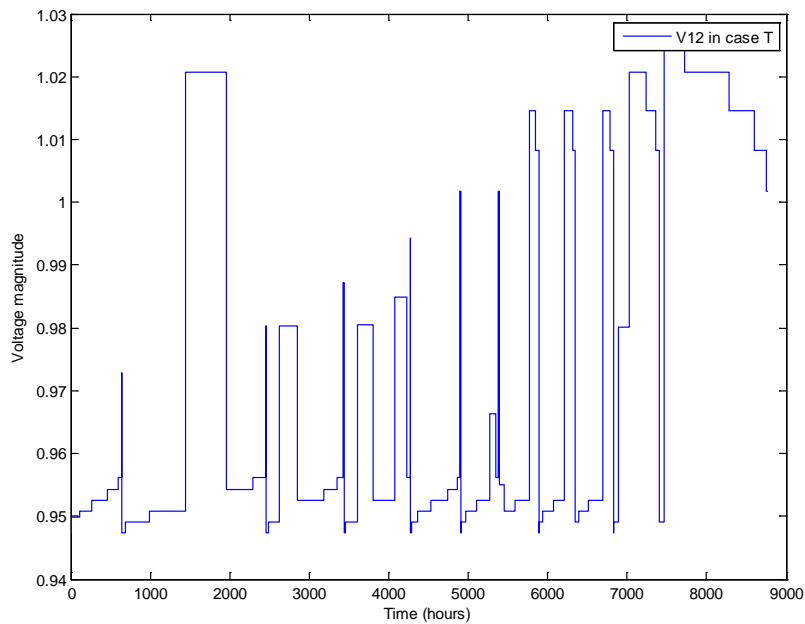


Figure 4-9: Voltage magnitude at bus 12 for case T

Comparison based on external reactive power support needed:

For case D, according to Figure 4-10, the system will need reactive power support at bus 2 and at bus 9 in order to keep the voltages at these buses fixed during all the periods and over the whole year and this is obvious because bus 2 and bus 9 are PV buses according to Table A- 2 in the appendices and also because there is no CVC in case D. On the other hand for case T, according to the results in Figure 4-11, there was need for extra reactive

power support for balancing the whole system at bus 2 only and this was coincidentally. For case D, there was need to try all the buses, one by one to choose the best bus to have reactive power support at it, and bus 2 was chosen because it resulted in the minimum DG capacity, while choosing reactive power support Q_c at other buses resulted higher DG capacity or no feasible solution.

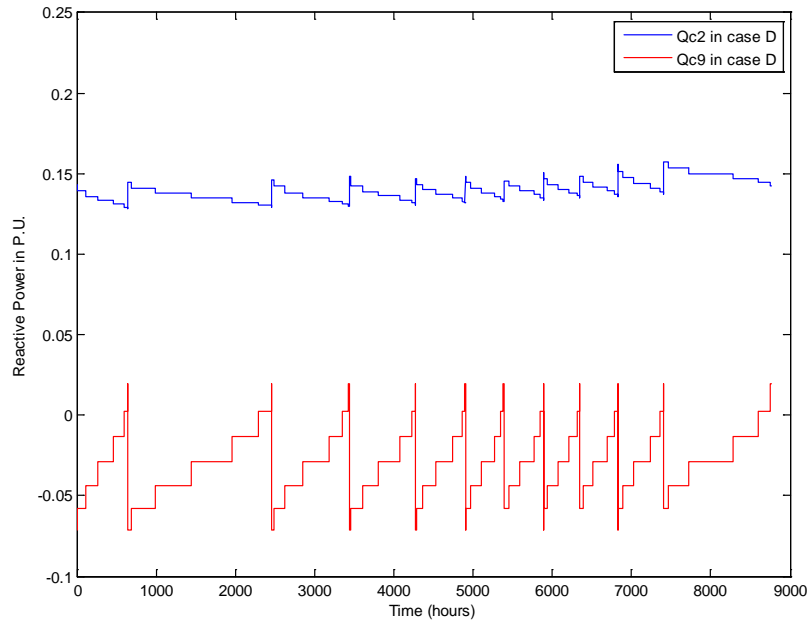


Figure 4-10: Reactive power support at bus 2 and bus 9 for case D

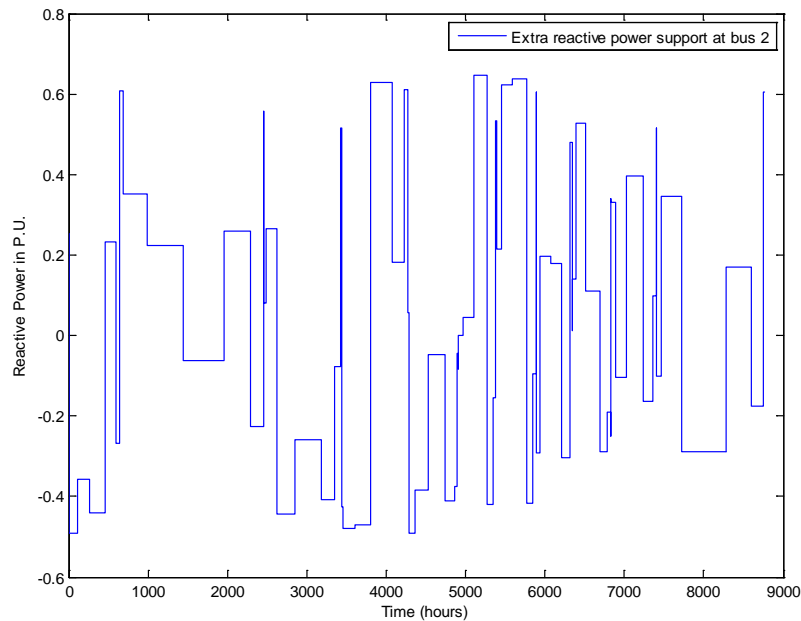


Figure 4-11: Extra reactive power support at bus 2 for case T.

Comparison based on active power curtailed:

Active wind energy curtailment was not used with case D and thus the curtailed power is zero during all the year for case D, on the other hand there is 10 % energy curtailment for case T and that energy curtailed will change from period to period according to Figure 4-12.

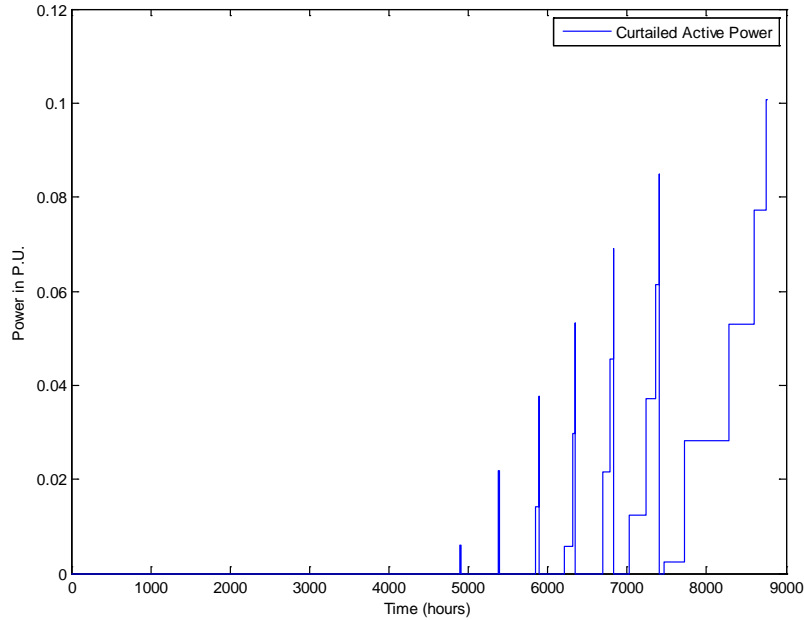


Figure 4-12: Active power curtailed in case T.

Comparison based on DG active power injection in the distribution network:

According to Figure 4-13, the active DG power injected into the distribution network in case T is always much higher than that in case D for every period and this is because case T has two extra active network schemes, CVC and 10 % energy curtailment, which case D doesn't have.

Comparison based on Slack active power:

Comparing the two cases regarding the active Slack bus power injected in the network, it can be seen that the active Slack bus power in case T is lower than the active Slack bus power in case D as seen from Figure 4-14 and this is obvious since the active DG power for case T was higher than the active DG power in case D.

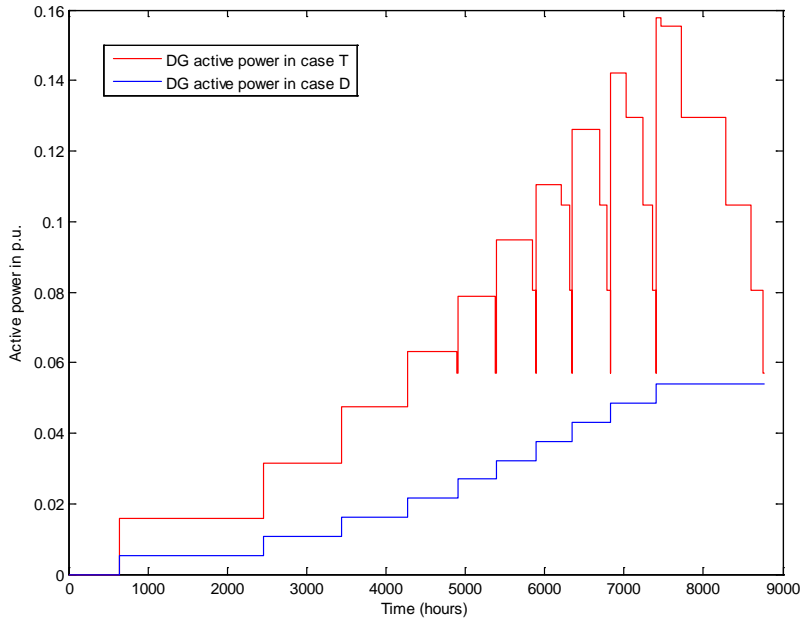


Figure 4-13: DG active power injection in both cases (D & T).

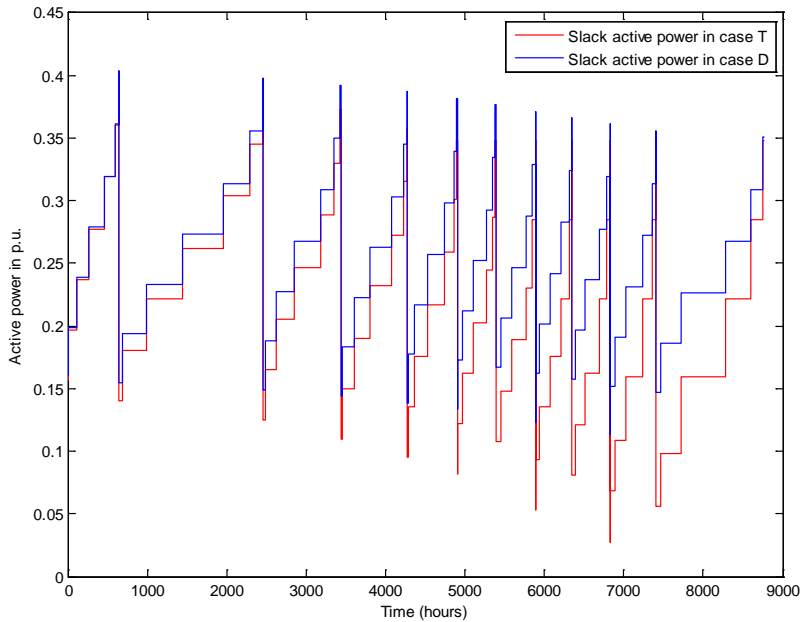


Figure 4-14: Slack bus active power injection in both cases.

Now with the same objective function of maximizing the DG capacity, the corresponding losses in MW for each case of the 20 cases is shown in Figure 4-15, from that figure, it can be seen that the losses with CVC are less than the cases without CVC (losses for cases A, B, C and D are less than that of cases E, F, G and H) and using energy curtailment as a control scheme tends to raise the energy losses, this is logically

understandable since the current in each case will face a larger resistance since the main power is coming from the DG which is not in an optimum location and less power is coming from the Slack bus.

Therefore, it can be said that even if the objective was to have the maximum DG capacity, the use of CVC as a control scheme reduces the energy losses significantly, while with using energy curtailment, the losses could be even higher than the case with passive management, and this rule will be used in the next chapter.

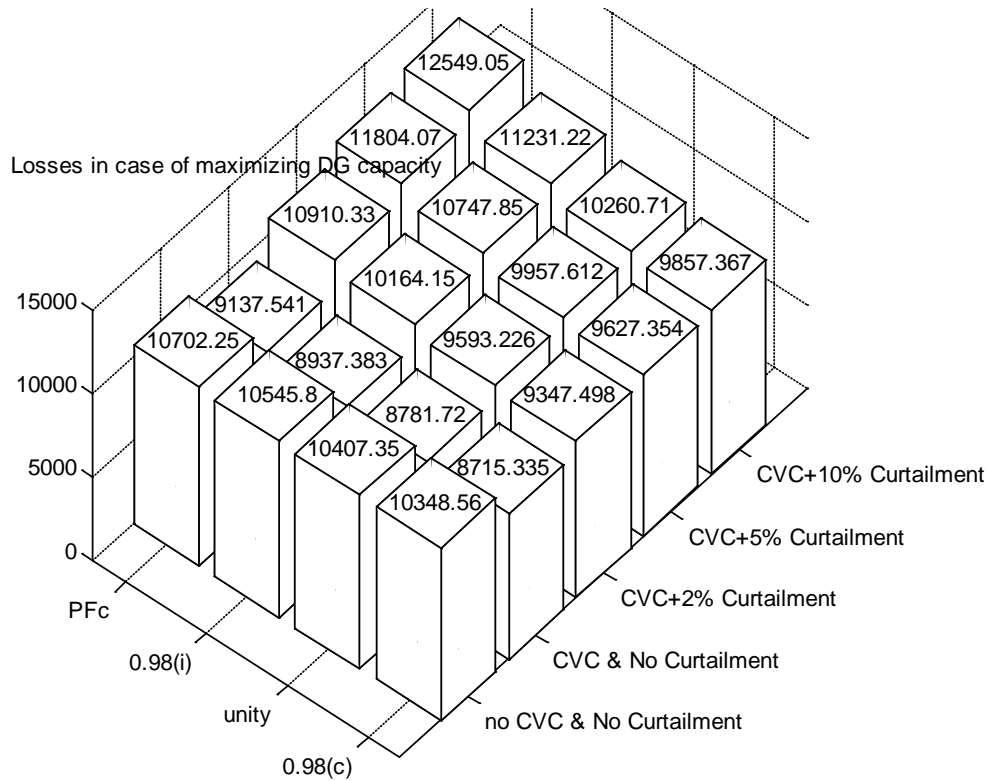


Figure 4-15: Losses in MWh in case of maximizing the DG capacity.

To summarize the main big differences between the 20 different, see Table 4-4:

Table 4-4: The main differences between the 20 different cases:

Comparing	No CVC & No Curtailment, Cases A, B, C and D	CVC & No Curtailment, cases E, F, G & H	CVC + Energy Curtailment, cases from I to T.
OLTC Secondary Voltage V_2	V_2 is held constant at 1.036 p.u for all periods (8760 hours) like a PV bus.	$0.94 \leq V_{2,m} \leq 1.06$ So V_2 changes for each period.	
Voltage Regulator secondary	V_9 is held constant at 1.03 p.u for all periods (8760 hours).	$0.94 \leq V_{9,m} \leq 1.06$ So V_9 changes for each period. (see figure)	

Voltage V_9			
Tapping of OLTC	The tapping of the OLTC is fixed at 0.97, during all periods.	A real continuous number between 0.85 and 1.05, minimum and maximum tapping position, for example for a certain period the tapping could be 0.901457)	
Tapping of VR	Fixed at 0.92, which is the starting tap ratio, during all periods.		
Reactive Support	Needs minimum extra reactive support $Q_{2,m}^C$ & $Q_{9,m}^C$ to keep the voltage at the secondaries of the OLTC and VR constant (as they are PV buses)	Needs minimum reactive support $Q_{2,m}^C$ only to balance the system and it is at bus 2 coincidentally after checking the best suitable bus.	
$p_{g,m}^{curt}$	0 always	0 always	There will be some periods during the year where: $p_{g,m}^{curt} \neq 0$
If P_g is to be maximized	P_g Ranges from 3.14% to 5.38%.	P_g Ranges from 3.32% to 5.7%.	P_g Range from 6.26% to 15.77%.
Losses if PG is to be maximized	Range from 10348 MWh to 10702MWh	(Lowest Losses) Range from 8715MWh to 9137MWh	(Highest Losses) Range from 9347MWh to 12549MWh.

4.3 Results and Analysis in Case of using DSM:

When it comes to applying equation (3-41), there are two alternatives:

- Either to use $f_{b,m}$ (Random Demand Curtailment factor at bus b during each certain period m) giving 74 values for each bus as there are 74 periods.
- Or using f_b (Random Demand Curtailment factor at bus b and fixed for all periods) giving only one f_b value at each bus.

Apply $f_{b,m}$, the results obtained in Figure 4-16 were obtained, it can be observed from the results that using DSM together with CVC can achieve higher DG capacity than using the passive management alone; the demand side management cases in Figure 4-16 with the energy curtailment cases in Figure 4-4 because one is concerned with energy curtailment of wind while the other is concerned with curtailing some of the power loads during their peaks at certain periods.

It is important to note that a 10% curtailable load as shown in Figure 4-16 means that $f^{max} = 0.1$ and that 20% curtailable Load means that $f^{max} = 0.2$ and so on.

It can be shown from Figure 4-16 that by increasing $f_{b,m}$, the DG capacity increases for all cases except for the last two inductive cases, because it seems that for the inductive cases there is a break point between 0.2% curtailable load and 30% curtailable load and that's why when $f_{b,m}$ has a limitation of 0.3 we find that the corresponding DG capacity is less than the case when $f_{b,m}$ has a limitation of 0.2.

It has been found that by using DSM as a control scheme, high values of optimal DG capacity cannot be reached, if case T in Figure 4-16 was compared with case T in Figure 4-4.

Considering the 2nd alternative, applying f_b (Random Demand Curtailment at bus b and fixed for all periods), the results shown in Figure 4-17 were obtained, here as the limitation on f_b increases, the maximum DG capacity increases as well for all the different cases. Comparing Figure 4-17 with Figure 4-16, we find that each case in Figure 4-17 has a different value than that corresponding to it Figure 4-16, hence, using f_b will give different results than if $f_{b,m}$ was used.

It is worth mentioning that each case in Figure 4-16 and Figure 4-17 where DSM is used as an ANM way, takes around one hour in solution on a AMD Phenom™ IIX4 945 processor with 3.00 GHZ and 8 GB RAM, this time is because each case has 7696 unknown nonlinear variables beside using a high accuracy as the final nonlinear feasibility tolerance used was 1e-006 and the nonlinear optimality tolerance used was 1e-007, plus the Multistart option was invoked and set to "5", The Multistart is a strategy that has proven successful in overcoming the problem of the solver stopping at local optimum points by restarting the NLP solver several times from different initial points. It is not uncommon for a different starting point to lead to a different local solution point. Thus, restarting from enough unique points, and saving the best local solution as we go, then we stand a much better chance of finding the true global solution. This solution strategy is referred to as Multistart [37].

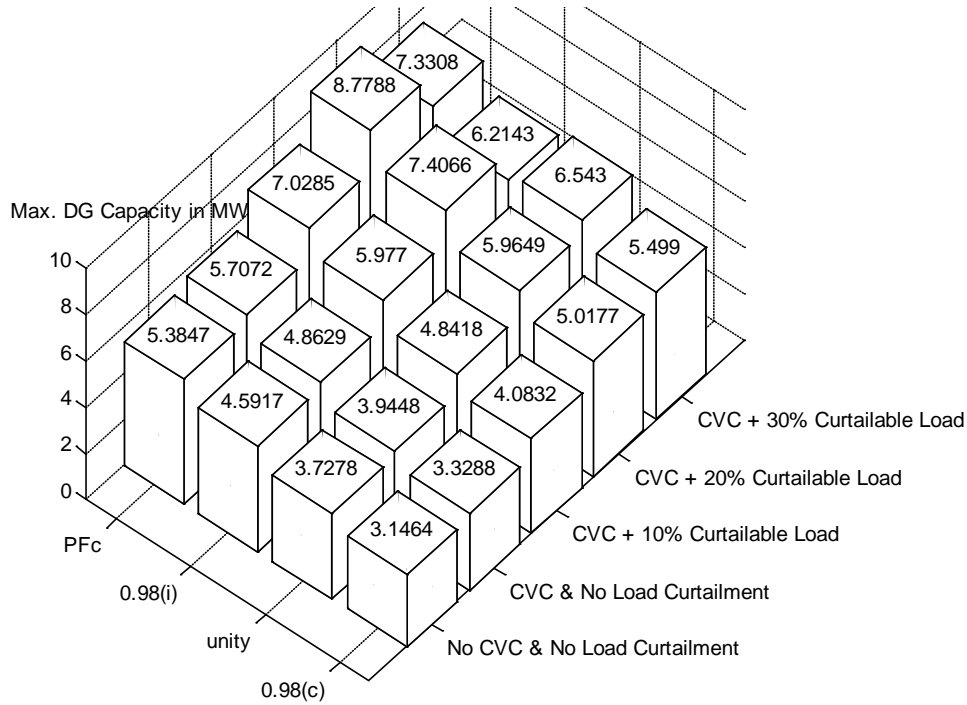


Figure 4-16: Maximum DG capacity in case of using DSM using Random Demand Curtailment factor at bus b during each certain period m .

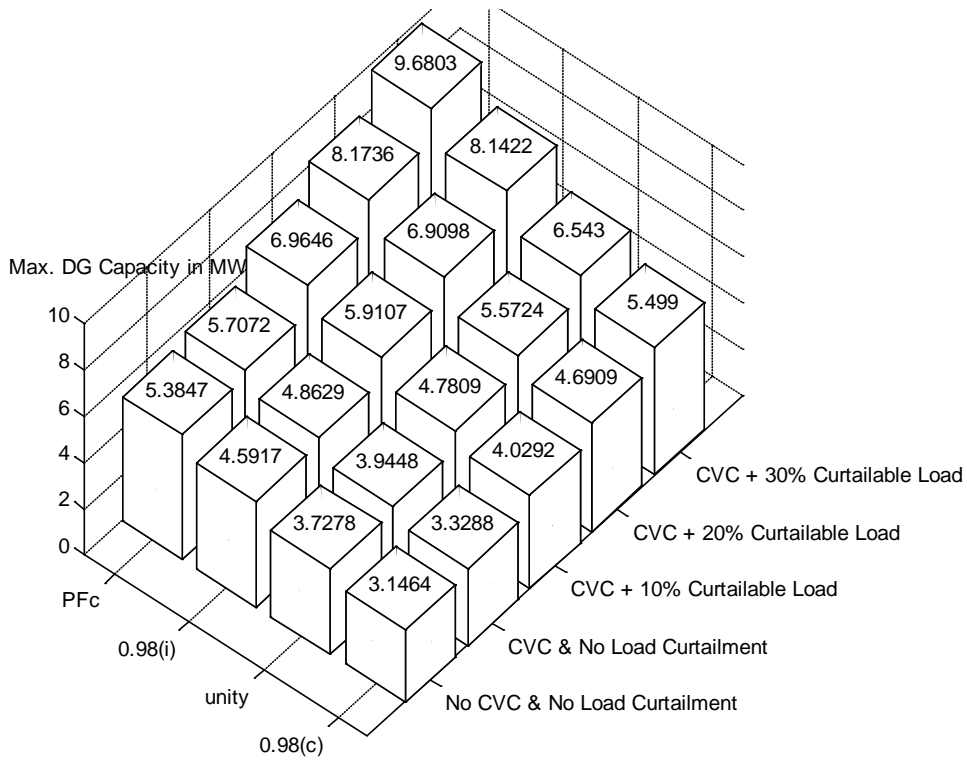


Figure 4-17: Max DG Capacity in case of using DSM with random demand curtailment factor at bus b and fixed for all periods.

5

Other Objective Functions and Load Growth Consideration

In this chapter the multi period AC OPF with different objective functions will be applied on the same case study used in chapter together with simplified analysis of the results. In addition to that, a separate study on the effect of load growth on the future DG capacity.

5.1 Minimizing the Losses

5.1.1 Introduction:

The problem of minimizing the losses in distribution networks has traditionally been investigated using a single, deterministic demand level. This has proved to be effective since most approaches are generally able to also result in minimum overall energy losses. However, the increasing penetration of intermittent distributed generation (DG) raises concerns on the actual benefits of loss minimization studies that are limited to a single demand/ generation scenario [35]. Here, a multiperiod AC optimal power flow (OPF) is used to determine the optimal accommodation of (renewable) DG in a way that minimizes the system energy losses.

Control schemes such as coordinated voltage control and dispatchable DG power factor only, are embedded in the OPF formulation to explore the extra loss reduction benefits that can be achieved with these control schemes.

The same previous generic U.K. distribution network is used as a case study and results demonstrate the gains that the control strategies can have on both loss minimization and generation capacity.

5.1.2 Formulating the Energy Loss Minimization Problem Using A Multi-period AC Optimal Power Flow:

The objective function of this loss analysis-focused AC OPF is the minimization of the total energy (line) losses over a given time horizon.

$$\min \sum_{m \in M} \left(\sum_{l \in L} f_{l,m}^{1,P} + f_{l,m}^{2,P} \right) \cdot \tau_m \quad (5-1)$$

The difference between the net injections at each end of the branch defines the energy loss. The objective is subject to a range of constraints which are exactly the same as in section 3.3.2 and the constraints regarding incorporating the adaptive power factor control (PFc) and coordinated voltage control (CVC) from equation (3-26) to equation (3-32), so there will be 8 cases only (A, B, to H)

It worth mentioning that in addition to the previously mentioned constraints, there is security, voltage step, and fault level constraints which can be implemented but are not considered here to ensure clarity. No capacity constraint is placed on the new DG units

since the aim is to accommodate as much capacity as is required to minimize the energy losses [35].

Applying this objective function to the previous example under study in chapter 4, the results obtained are shown in Figure 5-1, here, coordinated voltage control (CVC) and adaptive power factor control (PFc) have been implemented but generation curtailment was not, as the generation curtailment main purpose is to allow the connection of DG capacity beyond firm energy limit which tends to raise the energy losses, this was shown in the previous section and in [6, 35].

It can be seen from Figure 5-1 that the losses in cases A, B, C and D are the same and have a value of 10193.67 MWh, and the losses for cases E, F, G and H are the same with 8374.712 MWh as losses, thus, comparing case A with case E, or comparing case B with case F, or comparing case C with case F or case D with case H, it can be concluded that using CVC reduces the overall losses by 18 %, which is great, A summary of these results are represented in Table 5-1

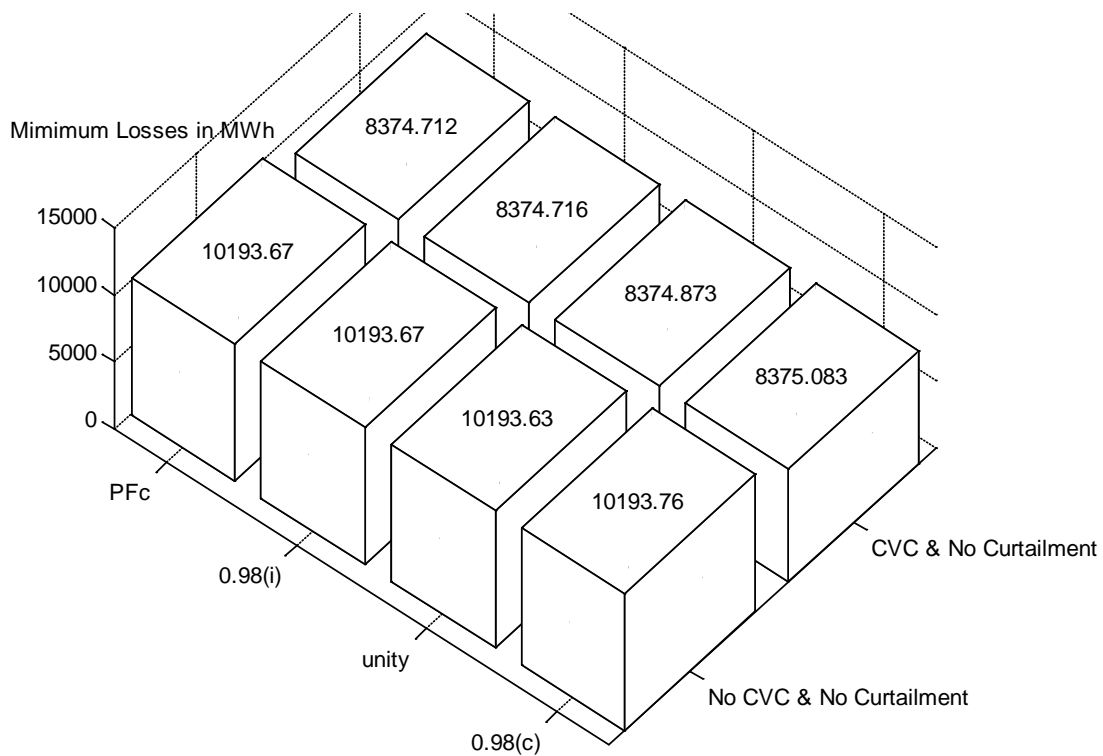


Figure 5-1: The minimum active energy losses.

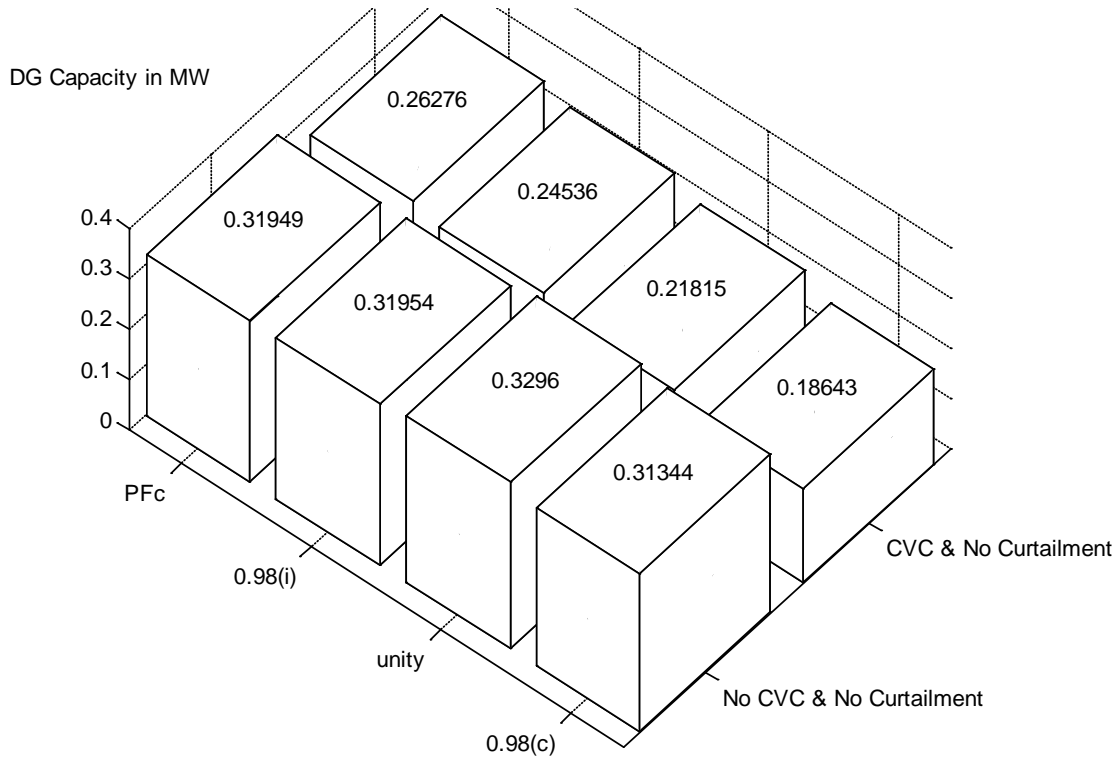


Figure 5-2: The corresponding DG capacity when the objective is to minimize the losses.

Table 5-1: Minimization of total energy losses and the 8 different cases.

Case	PF	CVC	Minimized losses in MWh	Corresponding DG capacity in MW
A	0.98 (c)	NO	10193.8	0.31344
B	1	NO	10193.8	0.3296
C	0.98 (i)	NO	10193.8	0.31954
D	PFc	NO	10193.8	0.31949
E	0.98 (c)	YES	8375	0.18643
F	1	YES	8375	0.21815
G	0.98 (i)	YES	8375	0.24536
H	PFc	YES	8375	0.26276

5.2 Trade-off between energy losses and renewable Energy

Although energy losses will remain as an imperative for DNOs to drive network performance-related investments, it is also true that more renewable generation is needed to achieve environmental targets. This creates a tension where, on one hand, modest DG capacities promote energy efficiency while, on the other hand, greater DG capacities deliver higher renewable production and network asset use. This can be evaluated by adapting the objective function to determine the generation capacity that maximizes the net energy from renewable sources [35], i.e., the harvested wind energy minus the energy losses:

$$\max \sum_{g \in G} \left(\sum_{m \in M} p_g \cdot w_m \cdot \tau_m \right) - \sum_{m \in M} \left(\sum_{l \in L} f_{l,m}^{1,P} + f_{l,m}^{2,P} \right) \cdot \tau_m \quad (5-2)$$

The objective is subject to a range of constraints which are exactly the same as in section 3.3.2 and the constraints regarding incorporating the adaptive power factor control (PFc) and coordinated voltage control (CVC) from equation (3-26) to equation (3-32), so there will be 8 cases only (A, B, to H).

The resulting trade-offs in terms of energy or the net maximized benefit between low-carbon energy and losses are presented in Figure 5-3 and the corresponding DG capacity for these cases is shown in Figure 5-4.

In Figure 5-3, coordinated voltage control (CVC) and adaptive power factor control (PFc) have been implemented but generation curtailment was not, as the generation curtailment main purpose is to allow the connection of DG capacity beyond firm energy limit which tends to raise the energy losses, this was shown in the previous section and [6, 35] and this is exactly the same as in the previous case of the energy loss minimization problem.

It can be seen from Figure 5-3 that the coordinated voltage control (CVC) gives better results than the passive network management and that PFc together with CVC gives better results than PFc alone.

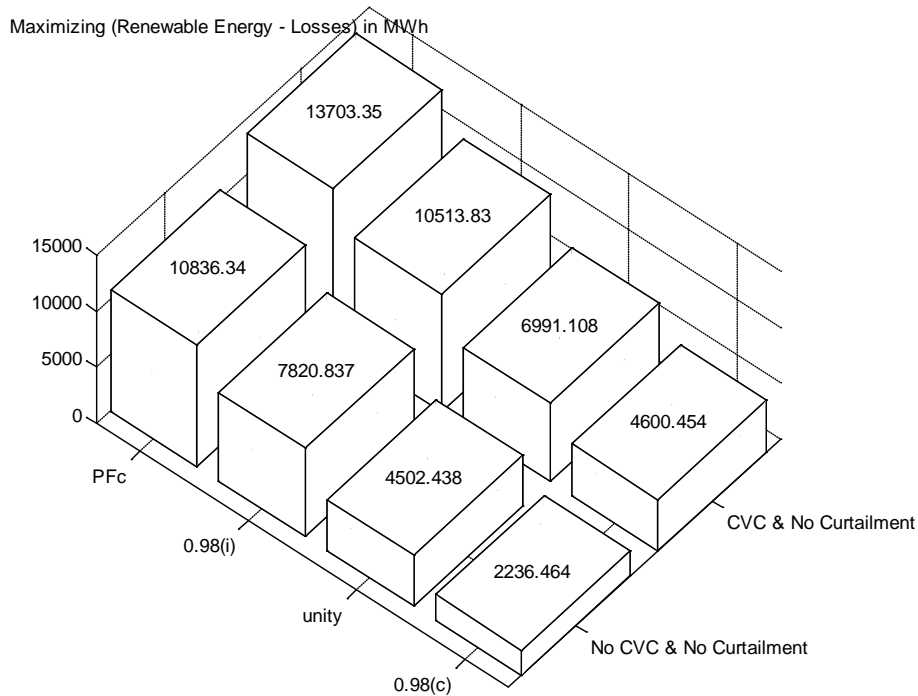


Figure 5-3: Net maximum (Renewable energy –losses) in MWh.

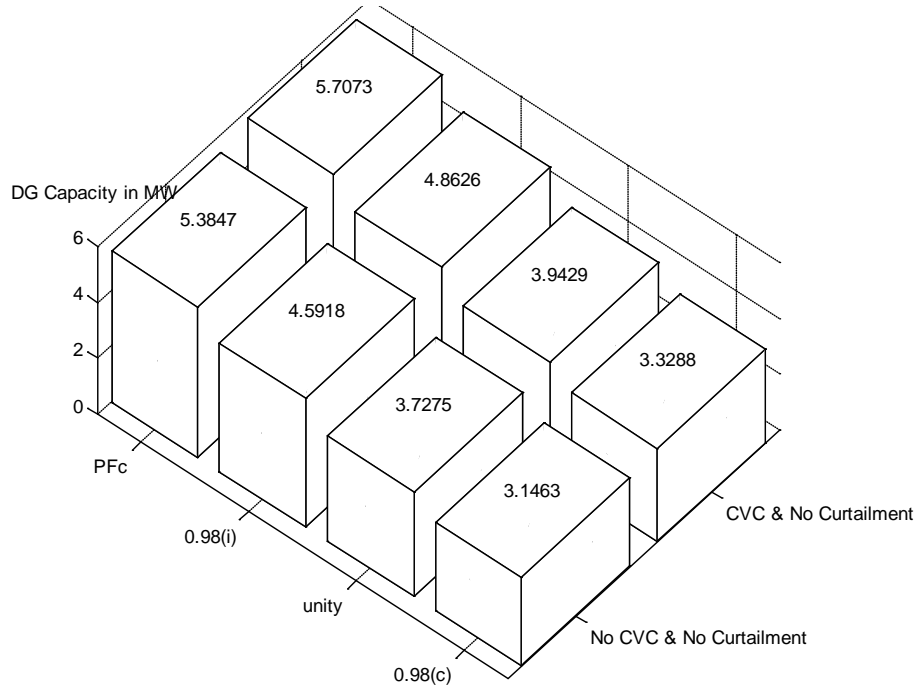


Figure 5-4: The corresponding DG capacity in case of maximizing the (Renewable energy – losses)

5.3 Minimizing the Total Average Voltage Deviation

The general equation of this objective function is:

$$\text{Min}[(1/(M \cdot B)) * 100 [\sum_{m=1}^{m=M} \sum_{b=1}^{b=B} |V_{b,m} - V_{b,nominal} |]] \quad (5-3)$$

Applying the above general equation to our previous case study example yields to:

$$\text{Min} \left[\left(\frac{100}{74 * 16} \right) \cdot \left[\sum_{m=1}^{m=74} (|V_{2,OLTC,m} - 1.036| + |V_{9,VR,m} - 1.03|) + \sum_{m=1}^{m=74} \sum_{\substack{b=1 \\ (b \neq 2, b \neq 9)}}^{b=16} |V_{b,m} - 1| \right] \right] \quad (5-4)$$

This objective function is to minimize the average deviation of the bus voltages from their nominal values, the results obtained are shown in Figure 5-5:

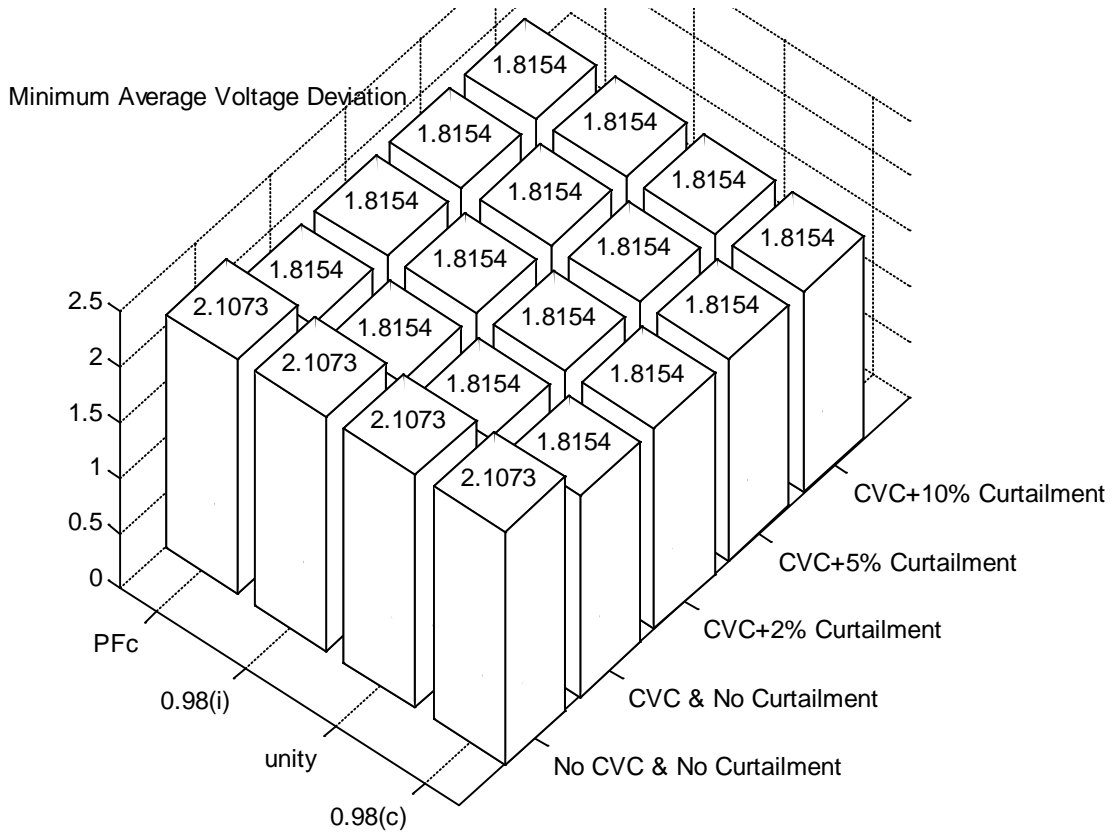


Figure 5-5: Minimum average voltage deviation.

It is clear that with implementation of ANM such as CVC, the average voltage deviation is reduced by 13.85%, and implementing energy curtailment will give the same results, the reason for that is that the DG capacity is zero and hence the DG active power is also zero also it seems that the location of the DG is not good because any power from DG will cause larger voltage drops on the lines compared with when power is extracted from the Slack bus, and hence larger deviation of bus voltages than their nominal.

5.4 Studying the effect of load growth

Assuming that the load growth factor is x and that the load increases by a factor of 7% annually such that by the end of the first next year the load becomes:

$$x \cdot d_b^P \eta_m \text{ \& \; } x \cdot d_b^Q \eta_m \quad (5-5)$$

Where:

$x \cdot d_b^P \eta_m$: is the active power at load bus b during the period m .

$x \cdot d_b^Q \eta_m$: is the reactive power at load bus b during the period m .

The model applied in this case is the same base model in section 3.3.1 to the end of section 3.4.3 but the load terms $d_b^P \eta_m$ & $d_b^Q \eta_m$ in equation (3-33),(3-34) and (3-35) have to be replaced with $x \cdot d_b^P \eta_m$ & $x \cdot d_b^Q \eta_m$.

For $x = 1.07$, the results obtained in this situation are shown in Figure 5-6, if the load continue to increase with the same rate in the next year by another 7%, that means that the load by the end of the 2nd year will be 1.14 higher than the original load or will have an $x = 1.14$, for a load growth of 14% the maximum DG capacity that can be reached in all 20 cases are gathered in Figure 5-7. It is worth mentioning that the limit of load increase is 14% and above that limit there will be no feasible solution for any case.

Comparing Figure 5-6 with Figure 4-4, it is clear that for all cases except A, B, C & D in Figure 5-6 the maximum DG capacity are less than their corresponding cases in Figure 4-4, and as:

- For all cases except A, B, C & D in the two figures, there is no reactive power support at bus 9 and the only reactive power support is at bus 2.
- In Figure 5-6 the system or network becomes more stressed.
- Almost all of the load points are close to the location of the slack bus than to the location of the DG.

The previous three main points explain that the active and reactive power would come from the slack bus rather than the DG and hence the maximum DG capacity is reduced as the system is more loaded.

But it is so important to mention that it is not a general rule because if the DG was more close to the load centers than the Slack bus then the DG capacity would increase as the load increases and that DG capacity would be limited only by the thermal limit of the cable connected to the DG.

When the load increases by 14%, the results are shown in Figure 5-7 were the highest maximum DG capacity that can be reached is 12.04 MW. Referring back to Figure 4-4 with the original load, it was found that the maximum DG capacity was 15.77 MW, so it is practical to say that it is more suitable to install 12.04 MW than to install 15.77 MW because that is going to save a lot of money specially when it is known that the load is going to increase up to a well-known limit.

The 12.04 MW capacity could be increased more by installing more reactive power support rather than that installed at bus 2, but this needs more reactive power support at the best bus. Finding the best bus requires solving the optimization problem several times, and in each case there is different location for the reactive power support bus and best location which gives the highest DG capacity. A cost benefit study comparing the cost of these additional reactive power support versus the cost of the extra DG capacity above the 12.04 MW decides if it worth it or not.

In other words, suppose that an extra additional reactive power support was chosen to be placed at bus 3, after optimization, the solution is z1, then another location for the

reactive power support is chosen, i.e. at bus 4, and after optimization the solution was found to be z2 and so on. The best solution is the highest value over all the available z's.

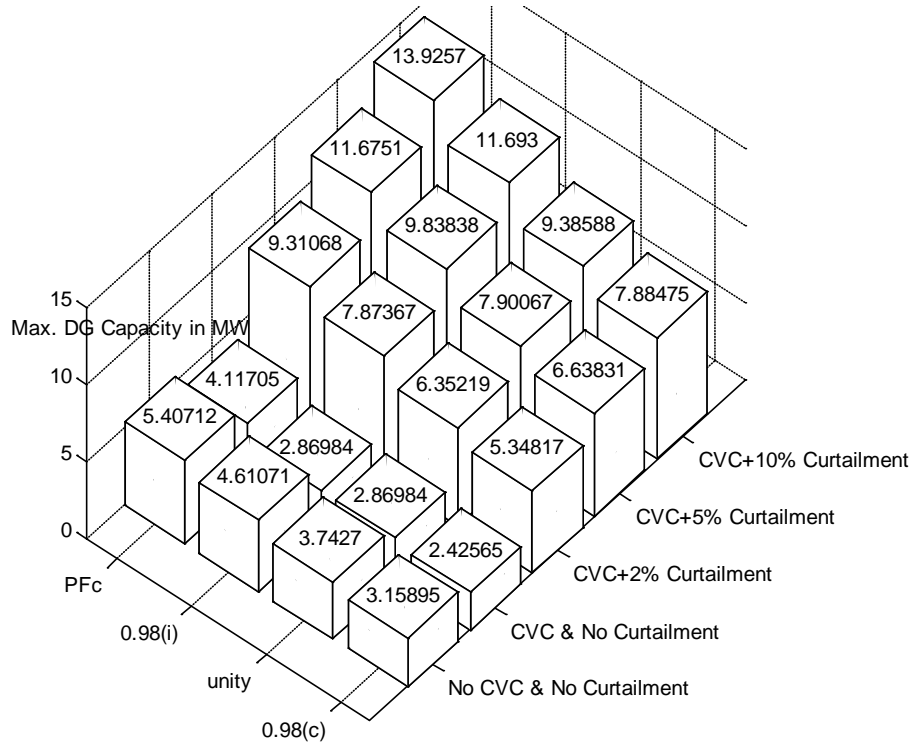


Figure 5-6: Maximum DG capacity for load increase by 7%.

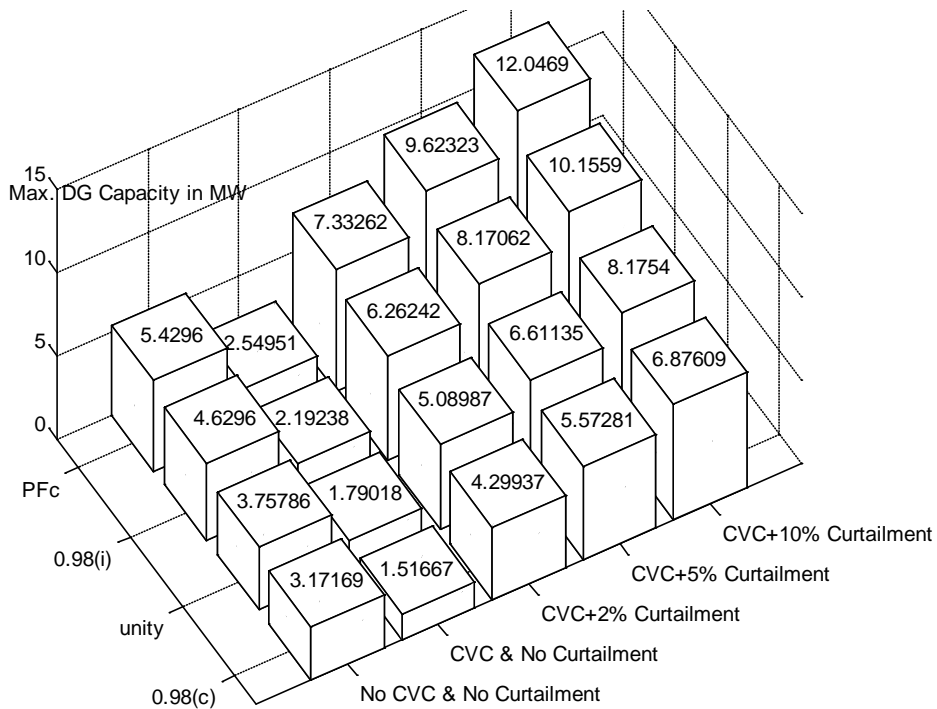


Figure 5-7: Maximum DG capacity for a load increase by 14%.

6

Conclusions and Future Works

6.1 Conclusions:

After this work, the following conclusions can be made:

- Passive distribution network operating philosophy tends to limit the amount of EWG that can be connected into the distribution network.
- By strategically adopting ANM schemes, very high penetration levels of new variable generation capacity can be reached when compared to the widely used passive operation of distribution networks.
- The Multi-period AC OPF-based technique was able to explore the maximum wind energy that can be delivered through network with different active management option and thus can be used to asses network operators during system planning processes.
- Generation curtailment main purpose is to allow the connection of DG capacity beyond distribution network limit which tends to raise the energy losses and thus when the objective is the minimization of the energy losses, the energy curtailment control scheme is not considered.
- The Multi-period AC OPF-based technique has demonstrated that optimal CVC combined with adequate power factor setting for the DG unit can lead to significant benefits in terms of loss reduction.
- It has been found that with ANM schemes, the average voltage deviation can be reduced.
- By increasing the level of the load power that can be curtailed, more DG capacity can be achieved.

6.2 Future Work:

It is important to carry out the following future work:

- In this thesis a 10% interval was used for simplicity, but the resolution can be increased, but there will be greater number of coincident periods and slower processing time for computation. It would be nice if a future study applies higher resolution. This is not likely to be a significant issue for smaller systems but will be a challenge for larger systems. Further work can be done on larger systems with higher resolution.
- Different sites, with each having a DG with different generation profile can be employed; the challenge of correctly representing their correlations

grows along with the number of coincident periods and consequent processing requirement.

- Using DSM together with energy storage as a combined ANM scheme to increase DG capacity with multi period OPF, especially in case of load growth and in a heavily loaded distribution network, can be a future study to compare its effectiveness with other ANM Schemes.
- Implementing the multi-period optimal AC power flow and using the same example but with the objective of minimizing the annual active DG generation curtailed.
- Incorporating more network constraints: more complex network constraints (irrespective of the objective function), such as fault levels, N-1 security and voltage step change. Although, they can be implemented within a multi-period framework, under the fact that these constraints are more important during worst-case scenarios, the formulation can be presented for the single-period analysis (index m is not used), implementation of these constraints on are given in [46] but a more suitable example other than the one used in this thesis would be a better option such as that in [46].

Appendices

A.1: Classification of Optimization Problems

Table A-1: Classification of optimization problems according to difficulty

Abbreviation	Class	Description
LP	Linear Program	All expressions are linear and the model contains no integer restrictions on the variables.
QP	Quadratic Program	All expressions are linear or quadratic, the model is convex, and there are no integer restrictions.
ILP	Integer Linear Program	All expressions are linear, and a subset of the variables is restricted to integer values.
IQP	Integer Quadratic Program	All expressions are either linear or quadratic, the model is convex, and a subset of the variables has integer restrictions.
PILP	Pure Integer Linear Program	All expressions are linear, and all variables are restricted to integer values.
PIQP	Pure Integer Quadratic Program	All expressions are linear or quadratic, the model is convex, and all variables are restricted to integer values.
NLP	Nonlinear Program	At least one of the relationships in the model is nonlinear with respect to the variables.
INLP	Integer Nonlinear Program	At least one of the expressions in the model is non-linear, and a subset of the variables has integer restrictions. In general, this class of model will be very difficult to solve for all but the smallest cases.
PINLP	Pure Integer Nonlinear Program	At least one of the expressions in the model is non-linear, and all variables have integer restrictions. In general, this class of model will be very difficult to solve for all but the smallest cases.

The LP is easier than QP and the most difficult is PINLP.

A.2: "Proof of power flow equations"

(Proof of Equations (3-11), (3-12), (3-13) and (3-14)):

The current I flowing in the direction from β_l^1 to β_l^2 is:

$$I_{\beta_l^1, \beta_l^2} = y_l * (V_{\beta_l^1} - V_{\beta_l^2}) + j \cdot \left(\frac{b_l^c}{2}\right) \cdot V_{\beta_l^1}$$

The complex power is :

$$S_l^1 = f_l^{1,P} + j \cdot f_l^{1,Q}$$

$$y_l = z_l^{-1} = g_l + j \cdot b_l$$

$$y_l^* = g_l - j \cdot b_l$$

$$S_l^1 = V_{\beta_l^1}^* \cdot I_{\beta_l^1, \beta_l^2}^* = y_l^* \cdot V_{\beta_l^1} \cdot e^{j\delta_{\beta_l^1}} \cdot (V_{\beta_l^1} \cdot e^{-j\delta_{\beta_l^1}} - V_{\beta_l^2} \cdot e^{-j\delta_{\beta_l^2}}) - j \cdot \left(\frac{b_l^C}{2}\right) \cdot V_{\beta_l^1}^2$$

$$S_l^1 = (g_l - j \cdot b_l) \cdot V_{\beta_l^1}^2 - (g_l - j \cdot b_l) \cdot V_{\beta_l^1} \cdot V_{\beta_l^2} \cdot e^{j(\delta_{\beta_l^1} - \delta_{\beta_l^2})} - j \cdot \left(\frac{b_l^C}{2}\right) \cdot V_{\beta_l^1}^2$$

$$S_l^1 = g_l \cdot V_{\beta_l^1}^2 - j \cdot b_l \cdot V_{\beta_l^1}^2 - g_l \cdot V_{\beta_l^1} \cdot V_{\beta_l^2} \cdot (\cos(\delta_{\beta_l^1} - \delta_{\beta_l^2}) + j \cdot \sin(\delta_{\beta_l^1} - \delta_{\beta_l^2})) \\ + j \cdot b_l \cdot V_{\beta_l^1} \cdot V_{\beta_l^2} (\cos(\delta_{\beta_l^1} - \delta_{\beta_l^2}) + j \cdot \sin(\delta_{\beta_l^1} - \delta_{\beta_l^2})) - j \cdot \left(\frac{b_l^C}{2}\right) \cdot V_{\beta_l^1}^2$$

$$S_l^1 = g_l \cdot V_{\beta_l^1}^2 - j \cdot b_l \cdot V_{\beta_l^1}^2 - g_l \cdot V_{\beta_l^1} \cdot V_{\beta_l^2} \cdot \cos(\delta_{\beta_l^1} - \delta_{\beta_l^2}) - j \cdot g_l \cdot V_{\beta_l^1} \cdot V_{\beta_l^2} \cdot \sin(\delta_{\beta_l^1} - \delta_{\beta_l^2}) \\ + j \cdot b_l \cdot V_{\beta_l^1} \cdot V_{\beta_l^2} \cdot \cos(\delta_{\beta_l^1} - \delta_{\beta_l^2}) - b_l \cdot V_{\beta_l^1} \cdot V_{\beta_l^2} \cdot \sin(\delta_{\beta_l^1} - \delta_{\beta_l^2}) \\ - j \cdot \left(\frac{b_l^C}{2}\right) \cdot V_{\beta_l^1}^2$$

Separating the real and imaginary parts in complex power equation:

$$f_l^{1,P} = g_l \cdot V_{\beta_l^1}^2 - V_{\beta_l^1} \cdot V_{\beta_l^2} \cdot (g_l \cdot \cos(\delta_{\beta_l^1} - \delta_{\beta_l^2}) + b_l \cdot \sin(\delta_{\beta_l^1} - \delta_{\beta_l^2}))$$

$$f_l^{1,Q} = -b_l \cdot V_{\beta_l^1}^2 - V_{\beta_l^1} \cdot V_{\beta_l^2} (g_l \cdot \sin(\delta_{\beta_l^1} - \delta_{\beta_l^2}) - b_l \cdot \cos(\delta_{\beta_l^1} - \delta_{\beta_l^2})) - \left(\frac{b_l^C}{2}\right) \cdot V_{\beta_l^1}^2$$

So when implementing the period index m on the last two equations we get:

$$f_{l,m}^{1,P} = g_l \cdot V_{\beta_{l,m}^1}^2 - V_{\beta_{l,m}^1} \cdot V_{\beta_{l,m}^2} \cdot [g_l \cdot \cos(\delta_{\beta_{l,m}^1} - \delta_{\beta_{l,m}^2}) + b_l \cdot \sin(\delta_{\beta_{l,m}^1} - \delta_{\beta_{l,m}^2})]$$

$$f_{l,m}^{1,Q} = -b_l \cdot V_{\beta_{l,m}^1}^2 - V_{\beta_{l,m}^1} \cdot V_{\beta_{l,m}^2} \cdot [g_l \cdot \sin(\delta_{\beta_{l,m}^1} - \delta_{\beta_{l,m}^2}) - b_l \cdot \cos(\delta_{\beta_{l,m}^1} - \delta_{\beta_{l,m}^2})] \\ - \left(\frac{b_l^C}{2}\right) \cdot V_{\beta_{l,m}^1}^2$$

The last term $\left(\frac{b_l^C}{2}\right) \cdot V_{\beta_{l,m}^1}^2$ in the equation can be cancelled since this term will be taken in reactive power balance at the corresponding bus, when the bus has a capacitive shunt connected to it as in equation (3-18), otherwise we can use the equation in the following form:

$$f_{l,m}^{1,Q} = -\left(b_l - \frac{b_l^C}{2}\right) \cdot V_{\beta_{l,m}^1}^2 - V_{\beta_{l,m}^1} \cdot V_{\beta_{l,m}^2} \cdot [g_l \cdot \sin(\delta_{\beta_{l,m}^1} - \delta_{\beta_{l,m}^2}) - b_l \cdot \cos(\delta_{\beta_{l,m}^1} - \delta_{\beta_{l,m}^2})]$$

The active and reactive power flows in the opposite direction $f_{l,m}^{2,P}$ and $f_{l,m}^{2,Q}$ can be obtained in the same previous way and will result in the same equations (3-13) and (3-14)

A.3: Data of the Simplified EHV1 Network from the U.K. Generic Distribution System (GDS)

i. Buses of the EHV1

Table A-2: Buses of the simplified EHV1 network.

Parameter	Base Voltage	Bus Type	Target Voltage Magnitude	Minimum Voltage	Maximum Voltage
Symbol	BBV	BTY	BTV	BVN	BVX
1	132	Slack	1	0.94	1.06
2	33	PV	1.036	0.94	1.03
3	33	PQ	1	0.94	1.06
4	33	PQ	1	0.94	1.06
5	33	PQ	1	0.94	1.06
6	33	PQ	1	0.94	1.06
7	33	PQ	1	0.94	1.06
8	33	PQ	1	0.94	1.06
9	33	PV	1.03	0.94	1.06
10	33	PQ	1	0.94	1.06
11	33	PQ	1	0.94	1.06
12	33	PQ	1	0.94	1.06
13	33	PQ	1	0.94	1.06
14	33	PQ	1	0.94	1.06
15	33	PQ	1	0.94	1.06
16	33	PQ	1	0.94	1.06

Where:

Base Voltage: BBV: The base voltage, in kV, of this bus.

Bus Type: BTY: This parameter must be consistent with other network components. It indicates the type of the bus within the load flow solution. Buses can be of the normal PQ type, of the PV type if they have a generator attached, or be the slack/reference bus.

Target Voltage Magnitude: BTV: A starting value and target value for voltage magnitude, in per unit. This may be set to 1 in the absence of other data. This value is used both as the starting value for the load flow solution and as the target value for

voltage control effected by generators, transformers and switched shunts. Thus, this value may form a part of data for other components when translated into proprietary formats.

Minimum Voltage: BVN: The minimum voltage allowed on this bus, in per unit. Some form of voltage control may be assigned to this bus, e.g. generator reactive power output or transformer tap position will be varied to keep the controlled bus voltage within limits.

Maximum Voltage: BVX: The maximum voltage allowed on this bus, in per unit. See above.

ii. Generators of the EHV1 Simplified Network

Table A-3: Generators of the EHV1 simplified network

Generator ID	Maximum Real Power	Minimum Real Power	Maximum Reactive Power	Minimum Reactive Power
GID	GPX	GPN	GQX	GQN
1	60	-60	60	-60

Generator ID: GID: A number that identifies individual generators if there is more than one on a single bus. Default to 1 if there is only one generator on the bus.

Maximum Real Power: GPX: The maximum limit of real power, in MW, used for assessing out-of-limit operation. A generator at the slack bus may go out of limits to solve the load flow.

Minimum Real Power: GPN: The minimum limit of real power, in MW. See above.

Maximum Reactive Power: GQX: The maximum reactive power output of the generator, in MVA_r. A generator with voltage control objectives will vary reactive power within its limits. If generator reactive power is to remain fixed (PQ-type operation) then this value should be set equal to the Reactive Power value.

Minimum Reactive Power: GQN: The minimum reactive power output of the generator, or the maximum reactive power absorbed by the generator, in MVA_r.

iii. Branches of the simplified EHV1 Network:

Table A-4: branches of the simplified EHV1 Network:

Index	From bus	To bus	R (p.u; 100 MVA)	X (p.u; 100 MVA)	B (p.u; 100 MVA)	Rating (MVA)	Length
1	2	3	0.198	0.446	0	25	12.05
2	2	4	0.187	0.299	0	45	18.48
3	3	4	0.216	0.287	0	20	8.79
4	4	5	0.0305	0.029	0.0015	40	2.055

Management of Active Distribution Networks with High Penetration of Distributed Generation

5	4	6	0.517	0.376	0	15	10.53
6	6	7	0.394	0.348	0	15	10.15
7	4	8	0.441	0.392	0.007	15	16.45
8	9	10	0.538	0.733	0	15	22.28
9	10	11	0.944	0.657	0	15	19.05
10	10	12	1.59	1.21	0.001	15	32.79
11	2	13	0.213	0.284	0	20	8.69
12	2	14	0.506	0.532	0.002	15	17.18
13	13	15	0.265	0.281	0.001	15	8.76
14	15	14	0.4	0.291	0	15	8.16
15	15	16	0.401	0.292	0	15	8.19
16	1	2	0	0.25	0	30	
17	1	2	0	0.25	0	30	
18	8	9	0.0728	0.1039	0	15	

iv. Transformers of the simplified EHV1 Network:

Table A-5: Transformers of the simplified EHV1 network

From Bus	TFB	1	1	8
To Bus	TTB	2	2	9
Transformer ID	TID	1	2	1
Positive and Negative Sequence Resistance	TR1	0	0	0.0728
Positive and Negative Sequence Reactance	TX1	0.25	0.25	0.1039
Zero Sequence Reactance	TX0	0.25	0.25	0
Earthing Resistance	TRE	50	50	0
Earthing Reactance	TXE	0	0	0
Iron Loss	TIL	0	0	0
Magnetizing Current	TMC	0	0	0
Rating One	TM1	30	30	15
Rating Two	TM2	33	33	16.5
Rating Three	TM3	15	15	7.5
Status	TST	1	1	1
Starting Tap Ratio	TTR	0.97	0.97	0.92
Maximum Tap Position	TTX	1.05	1.05	1.05
Minimum Tap Position	TTN	0.85	0.85	0.85
Tap Positions	TTP	21	21	21
Winding Connection	TWC	DY	DY	DD
Phase Shift Angle	TPS	-30	-30	0
Controlled Bus	TCB	2	2	9

Explanation:

From Bus: TFB: Identifies the bus at the "from" end of the transformer.

To Bus: TTB: Identifies the bus at the "to" end of the transformer.

Transformer ID: TID: A number that identifies individual transformers if there is more than one connected between the same two buses. Default to 1 if there is only one transformer between these buses.

Positive and Negative Sequence Resistance: TR1: The positive and negative sequence resistances of the transformer should be the same value. This should be expressed in per unit on system base.

Positive and Negative Sequence Reactance: TX1: The positive and negative sequence reactances of the transformer should be the same value. This should be expressed in per unit on system base.

Zero Sequence Resistance: TR0: The zero sequence resistance of the transformer. This should be expressed in per unit on system base.

Zero Sequence Reactance: TX0: The zero sequence reactance of the transformer. This should be expressed in per unit on system base.

Earthing Resistance: TRE: The earthing resistance of the transformer. This should be expressed in per unit on system base. The role of earthing impedance in fault studies is influenced by the transformed Winding Connection (TWC).

Earthing Reactance: TXE: The earthing reactance of the transformer. This should be expressed in per unit on system base. The role of earthing impedance in fault studies is influenced by the transformed Winding Connection (TWC).

Iron Loss: TIL: The no load iron loss in the transformer core, expressed in Watts.

Magnetizing Current: TMC: The magnetizing current in per unit on system MVA base and nominal primary voltage base.

Rating One: TM1: Each transformer can be assigned three ratings in MVA. These will be used to assess overloads but may be interpreted in different ways by different software packages.

Rating Two: TM2: See above

Rating Three: TM3: See above

Status: TST: The transformer can be switched on (1) and off (0).

Starting Tap Ratio: TTR: The starting point for the transformer tap changer as a per unit nominal ratio. This value can be set to 1 in the absence of other data.

Maximum Tap Position: TTX: The maximum tap position as a per unit nominal value. The max and min tap position can be set equal to the starting ratio to indicate a fixed-tap transformer.

Minimum Tap Position: TTN: The minimum tap position as a per unit nominal value. The max and min tap position can be set equal to the starting ratio to indicate a fixed-tap transformer.

Tap Positions: TTP: The number of tap positions. This should be consistent with the maximum, minimum and starting tap positions.

Winding Connection: TWC: The transformer winding connection: YY, YD, DY or DD. This influences the zero sequence representation of the transformer for fault level studies. This does not influence the transformer phase shift angle (TPS), which must be specified separately.

Phase Shift Angle: TPS: The transformer phase shift angle in degrees.

Controlled Bus: TCB: The bus where the voltage is being controlled by changes in transformer tap position. Zero indicates that the controlled bus is the "To Bus" of the transformer. A negative number indicates that no bus is being controlled. Reference is made to the relevant bus data to determine the target, minimum and maximum voltage values.

v. Peak loads at the buses of the simplified EHV1 Network:

Table A-6: Peak active and reactive Load at each bus of the simplified EHV1 Network

Bus index	Peak Active Demand	Peak Reactive Demand
1	0	0
2	5.41	1.09
3	1.93	0.39
4	0.06	0.01
5	18.4	3.74
6	1.96	0.4
7	1.90	0.39
8	0	0
9	0.55	0.11
10	2.7	0.55
11	2.85	0.58
12	0.81	0.16
13	1.01	0.2
14	0.58	0.12
15	0	0
16	0	0

A.4: Data entry and implementation of case study of maximizing the DG capacity

Table A-7: Percent of peak demand and percent of generation capacity during each period.

$\tau_1 = 10$ $\eta_1 = 0.4$ $w_1 = 0$	$\tau_2 = 103$ $\eta_2 = 0.5$ $w_2 = 0$	$\tau_3 = 158$ $\eta_3 = 0.6$ $w_3 = 0$	$\tau_4 = 192$ $\eta_4 = 0.7$ $w_4 = 0$	$\tau_5 = 127$ $\eta_5 = 0.8$ $w_5 = 0$	$\tau_6 = 53$ $\eta_6 = 0.9$ $w_6 = 0$	$\tau_7 = 2$ $\eta_7 = 1$ $w_7 = 0$	0%	% of Generation Capacity
$\tau_8 = 43$ $\eta_8 = 0.4$ $w_8 = 0.1$	$\tau_9 = 303$ $\eta_9 = 0.5$ $w_9 = 0.1$	$\tau_{10} = 451$ $\eta_{10} = 0.6$ $w_{10} = 0.1$	$\tau_{11} = 515$ $\eta_{11} = 0.7$ $w_{11} = 0.1$	$\tau_{12} = 339$ $\eta_{12} = 0.8$ $w_{12} = 0.1$	$\tau_{13} = 156$ $\eta_{13} = 0.9$ $w_{13} = 0.1$	$\tau_{14} = 11$ $\eta_{14} = 1$ $w_{14} = 0.1$	10%	
$\tau_{15} = 20$ $\eta_{15} = 0.4$ $w_{15} = 0.2$	$\tau_{16} = 136$ $\eta_{16} = 0.5$ $w_{16} = 0.2$	$\tau_{17} = 226$ $\eta_{17} = 0.6$ $w_{17} = 0.2$	$\tau_{18} = 336$ $\eta_{18} = 0.7$ $w_{18} = 0.2$	$\tau_{19} = 175$ $\eta_{19} = 0.8$ $w_{19} = 0.2$	$\tau_{20} = 73$ $\eta_{20} = 0.9$ $w_{20} = 0.2$	$\tau_{21} = 15$ $\eta_{21} = 1$ $w_{21} = 0.2$	20%	
$\tau_{22} = 16$ $\eta_{22} = 0.4$ $w_{22} = 0.3$	$\tau_{23} = 147$ $\eta_{23} = 0.5$ $w_{23} = 0.3$	$\tau_{24} = 201$ $\eta_{24} = 0.6$ $w_{24} = 0.3$	$\tau_{25} = 276$ $\eta_{25} = 0.7$ $w_{25} = 0.3$	$\tau_{26} = 138$ $\eta_{26} = 0.8$ $w_{26} = 0.3$	$\tau_{27} = 45$ $\eta_{27} = 0.9$ $w_{27} = 0.3$	$\tau_{28} = 6$ $\eta_{28} = 1$ $w_{28} = 0.3$	30%	
$\tau_{29} = 11$ $\eta_{29} = 0.4$ $w_{29} = 0.4$	$\tau_{30} = 79$ $\eta_{30} = 0.5$ $w_{30} = 0.4$	$\tau_{31} = 170$ $\eta_{31} = 0.6$ $w_{31} = 0.4$	$\tau_{32} = 212$ $\eta_{32} = 0.7$ $w_{32} = 0.4$	$\tau_{33} = 113$ $\eta_{33} = 0.8$ $w_{33} = 0.4$	$\tau_{34} = 41$ $\eta_{34} = 0.9$ $w_{34} = 0.4$	$\tau_{35} = 4$ $\eta_{35} = 1$ $w_{35} = 0.4$	40%	
$\tau_{36} = 7$ $\eta_{36} = 0.4$ $w_{36} = 0.5$	$\tau_{37} = 63$ $\eta_{37} = 0.5$ $w_{37} = 0.5$	$\tau_{38} = 130$ $\eta_{38} = 0.6$ $w_{38} = 0.5$	$\tau_{39} = 161$ $\eta_{39} = 0.7$ $w_{39} = 0.5$	$\tau_{40} = 84$ $\eta_{40} = 0.8$ $w_{40} = 0.5$	$\tau_{41} = 33$ $\eta_{41} = 0.9$ $w_{41} = 0.5$	$\tau_{42} = 7$ $\eta_{42} = 1$ $w_{42} = 0.5$	50%	
0	$\tau_{43} = 60$ $\eta_{43} = 0.5$ $w_{43} = 0.6$	$\tau_{44} = 147$ $\eta_{44} = 0.6$ $w_{44} = 0.6$	$\tau_{45} = 172$ $\eta_{45} = 0.7$ $w_{45} = 0.6$	$\tau_{46} = 85$ $\eta_{46} = 0.8$ $w_{46} = 0.6$	$\tau_{47} = 41$ $\eta_{47} = 0.9$ $w_{47} = 0.6$	$\tau_{48} = 4$ $\eta_{48} = 1$ $w_{48} = 0.6$	60%	
$\tau_{49} = 1$ $\eta_{49} = 0.4$ $w_{49} = 0.7$	$\tau_{50} = 40$ $\eta_{50} = 0.5$ $w_{50} = 0.7$	$\tau_{51} = 132$ $\eta_{51} = 0.6$ $w_{51} = 0.7$	$\tau_{52} = 143$ $\eta_{52} = 0.7$ $w_{52} = 0.7$	$\tau_{53} = 95$ $\eta_{53} = 0.8$ $w_{53} = 0.7$	$\tau_{54} = 33$ $\eta_{54} = 0.9$ $w_{54} = 0.7$	$\tau_{55} = 4$ $\eta_{55} = 1$ $w_{55} = 0.7$	70%	
0	$\tau_{56} = 48$ $\eta_{56} = 0.5$ $w_{56} = 0.8$	$\tau_{57} = 123$ $\eta_{57} = 0.6$ $w_{57} = 0.8$	$\tau_{58} = 176$ $\eta_{58} = 0.7$ $w_{58} = 0.8$	$\tau_{59} = 90$ $\eta_{59} = 0.8$ $w_{59} = 0.8$	$\tau_{60} = 42$ $\eta_{60} = 0.9$ $w_{60} = 0.8$	$\tau_{61} = 8$ $\eta_{61} = 1$ $w_{61} = 0.8$	80%	
$\tau_{62} = 2$ $\eta_{62} = 0.4$ $w_{62} = 0.9$	$\tau_{63} = 54$ $\eta_{63} = 0.5$ $w_{63} = 0.9$	$\tau_{64} = 144$ $\eta_{64} = 0.6$ $w_{64} = 0.9$	$\tau_{65} = 212$ $\eta_{65} = 0.7$ $w_{65} = 0.9$	$\tau_{66} = 110$ $\eta_{66} = 0.8$ $w_{66} = 0.9$	$\tau_{67} = 48$ $\eta_{67} = 0.9$ $w_{67} = 0.9$	$\tau_{68} = 6$ $\eta_{68} = 1$ $w_{68} = 0.9$	90%	
0	$\tau_{69} = 63$ $\eta_{69} = 0.5$ $w_{69} = 1$	$\tau_{70} = 257$ $\eta_{70} = 0.6$ $w_{70} = 1$	$\tau_{71} = 559$ $\eta_{71} = 0.7$ $w_{71} = 1$	$\tau_{72} = 305$ $\eta_{72} = 0.7$ $w_{72} = 1$	$\tau_{73} = 152$ $\eta_{73} = 0.7$ $w_{73} = 1$	$\tau_{74} = 16$ $\eta_{74} = 0.7$ $w_{74} = 1$	100%	
40%	50%	60%	70%	80%	90%	100%		
% of Peak Demand								

$$MVA_{Base} = 100;$$

Table A-8: Values of Conductance, susceptance, shunt susceptance and line limits

$g_1 = 0.8315$	$b_1 = -1.8730$	$b_1^C = 0$	$f_1^+ = 25/MVA_{Base}$
$g_2 = 1.5036$	$b_2 = -2.4041$	$b_2^C = 0$	$f_2^+ = 45/MVA_{Base}$
$g_3 = 1.6741$	$b_3 = -2.2244$	$b_3^C = 0$	$f_3^+ = 20/MVA_{Base}$
$g_4 = 17.2195$	$b_4 = -16.3726$	$b_4^C = 0.0015$	$f_4^+ = 40/MVA_{Base}$
$g_5 = 1.2651$	$b_5 = -0.9201$	$b_5^C = 0$	$f_5^+ = 15/MVA_{Base}$
$g_6 = 1.4258$	$b_6 = -1.2593$	$b_6^C = 0$	$f_6^+ = 15/MVA_{Base}$
$g_7 = 1.2667$	$b_7 = -1.1260$	$b_7^C = 0.007$	$f_7^+ = 15/MVA_{Base}$
$g_8 = 0.6508$	$b_8 = -0.8866$	$b_8^C = 0$	$f_8^+ = 15/MVA_{Base}$
$g_9 = 0.7136$	$b_9 = -0.4967$	$b_9^C = 0$	$f_9^+ = 15/MVA_{Base}$
$g_{10} = 0.3983$	$b_{10} = -0.3031$	$b_{10}^C = 0.001$	$f_{10}^+ = 15/MVA_{Base}$
$g_{11} = 1.6901$	$b_{11} = -2.2535$	$b_{11}^C = 0$	$f_{11}^+ = 20/MVA_{Base}$
$g_{12} = 0.9387$	$b_{12} = -0.9869$	$b_{12}^C = 0.002$	$f_{12}^+ = 15/MVA_{Base}$
$g_{13} = 1.7763$	$b_{13} = -1.8836$	$b_{13}^C = 0.001$	$f_{13}^+ = 15/MVA_{Base}$
$g_{14} = 1.6348$	$b_{14} = -1.1893$	$b_{14}^C = 0$	$f_{14}^+ = 15/MVA_{Base}$
$g_{15} = 1.6297$	$b_{15} = -1.1867$	$b_{15}^C = 0$	$f_{15}^+ = 15/MVA_{Base}$
$g_{16} = 0$	$b_{16} = -4$	$b_{16}^C = 0$	$f_{16}^+ = 30/MVA_{Base}$
$g_{17} = 0$	$b_{17} = -4$	$b_{17}^C = 0$	$f_{17}^+ = 30/MVA_{Base}$
$g_{18} = 4.5231$	$b_{18} = -6.4554$	$b_{18}^C = 0$	$f_{18}^+ = 15/MVA_{Base}$

And the maximum active and reactive demand at each bus is:

Table A-9: Peak active and reactive power at each bus in the EHV1 network:

$d_2^P = 5.41/MVA_{Base}$	$d_2^Q = 1.09/MVA_{Base}$
$d_3^P = 1.93/MVA_{Base}$	$d_3^Q = 0.39/MVA_{Base}$
$d_4^P = 0.06/MVA_{Base}$	$d_4^Q = 0.01/MVA_{Base}$
$d_5^P = 18.4/MVA_{Base}$	$d_5^Q = 3.74/MVA_{Base}$
$d_6^P = 1.96/MVA_{Base}$	$d_6^Q = 0.40/MVA_{Base}$
$d_7^P = 1.90/MVA_{Base}$	$d_7^Q = 0.39/MVA_{Base}$
$d_8^P = 0$	$d_8^Q = 0$
$d_9^P = 0.55/MVA_{Base}$	$d_9^Q = 0.11/MVA_{Base}$
$d_{10}^P = 2.70/MVA_{Base}$	$d_{10}^Q = 0.55/MVA_{Base}$
$d_{11}^P = 2.85/MVA_{Base}$	$d_{11}^Q = 0.58/MVA_{Base}$
$d_{12}^P = 0.81/MVA_{Base}$	$d_{12}^Q = 0.16/MVA_{Base}$
$d_{13}^P = 1.01/MVA_{Base}$	$d_{13}^Q = 0.20/MVA_{Base}$
$d_{14}^P = 0.58/MVA_{Base}$	$d_{14}^Q = 0.12/MVA_{Base}$
$d_{15}^P = 0$	$d_{15}^Q = 0$
$d_{16}^P = 0$	$d_{16}^Q = 0$

A.5: Implementation

i. Line flows on lines and transformers:

$\forall m \in M$ and $\forall l \in L$:

Applying equations (3-11), (3-12), (3-13) and (3-14):

For line 1:

$$f_{1,m}^{1,P} = g_1 \cdot V_{2,m}^2 - V_{2,m} \cdot V_{3,m} \cdot [g_1 \cdot \cos(\delta_{2,m} - \delta_{3,m}) + b_1 \cdot \sin(\delta_{2,m} - \delta_{3,m})]$$

$$f_{1,m}^{1,Q} = -b_1 \cdot V_{2,m}^2 - V_{2,m} \cdot V_{3,m} \cdot [g_1 \cdot \sin(\delta_{2,m} - \delta_{3,m}) - b_1 \cdot \cos(\delta_{2,m} - \delta_{3,m})]$$

$$f_{1,m}^{2,P} = g_1 \cdot V_{3,m}^2 - V_{3,m} \cdot V_{2,m} \cdot [g_1 \cdot \cos(\delta_{3,m} - \delta_{2,m}) + b_1 \cdot \sin(\delta_{3,m} - \delta_{2,m})]$$

$$f_{1,m}^{2,Q} = -b_1 \cdot V_{3,m}^2 - V_{3,m} \cdot V_{2,m} \cdot [g_1 \cdot \sin(\delta_{3,m} - \delta_{2,m}) - b_1 \cdot \cos(\delta_{3,m} - \delta_{2,m})]$$

Then for $b = 2$ to 15 in the same manner to get $f_{b,m}^{1,P}$, $f_{b,m}^{2,P}$, $f_{b,m}^{1,Q}$ and $f_{b,m}^{2,Q}$

The first OLTC (line 16):

$$f_{16,m}^{1,P} = g_{16} \cdot \left(\frac{V_{1,m}}{T_{OLTC,m}}\right)^2 - \left(\frac{V_{1,m}}{T_{OLTC,m}}\right) \cdot V_{2,m} \cdot [g_{16} \cdot \cos(\delta_{1,m} - \delta_{2,m}) + b_{16} \cdot \sin(\delta_{1,m} - \delta_{2,m})]$$

$$f_{16,m}^{1,Q} = -b_{16} \cdot \left(\frac{V_{1,m}}{T_{OLTC,m}}\right)^2 - \left(\frac{V_{1,m}}{T_{OLTC,m}}\right) \cdot V_{2,m} \cdot [g_{16} \cdot \sin(\delta_{1,m} - \delta_{2,m}) - b_{16} \cdot \cos(\delta_{1,m} - \delta_{2,m})]$$

$$f_{16,m}^{2,P} = g_{16} \cdot V_{2,m}^2 - V_{2,m} \cdot \left(\frac{V_{1,m}}{T_{OLTC,m}}\right) \cdot [g_{16} \cdot \cos(\delta_{2,m} - \delta_{1,m}) + b_{16} \cdot \sin(\delta_{2,m} - \delta_{1,m})]$$

$$f_{16,m}^{2,Q} = -b_{16} \cdot V_{2,m}^2 - V_{2,m} \cdot \left(\frac{V_{1,m}}{T_{OLTC,m}}\right) \cdot [g_{16} \cdot \sin(\delta_{2,m} - \delta_{1,m}) - b_{16} \cdot \cos(\delta_{2,m} - \delta_{1,m})]$$

The 2nd OLTC (line 17):

$$f_{17,m}^{1,P} = g_{17} \cdot \left(\frac{V_{1,m}}{T_{OLTC,m}}\right)^2 - \left(\frac{V_{1,m}}{T_{OLTC,m}}\right) \cdot V_{2,m} \cdot [g_{17} \cdot \cos(\delta_{1,m} - \delta_{2,m}) + b_{17} \cdot \sin(\delta_{1,m} - \delta_{2,m})]$$

$$f_{17,m}^{1,Q} = -b_{17} \cdot \left(\frac{V_{1,m}}{T_{OLTC,m}} \right)^2 - \left(\frac{V_{1,m}}{T_{OLTC,m}} \right) \cdot V_{2,m} \cdot [g_{17} \cdot \sin(\delta_{1,m} - \delta_{2,m}) - b_{17} \cdot \cos(\delta_{1,m} - \delta_{2,m})]$$

$$f_{17,m}^{2,P} = g_{17} \cdot V_{2,m}^2 - V_{2,m} \cdot \left(\frac{V_{1,m}}{T_{OLTC,m}} \right) \cdot [g_{17} \cdot \cos(\delta_{2,m} - \delta_{1,m}) + b_{17} \cdot \sin(\delta_{2,m} - \delta_{1,m})]$$

$$f_{17,m}^{2,Q} = -b_{17} \cdot V_{2,m}^2 - V_{2,m} \cdot \left(\frac{V_{1,m}}{T_{OLTC,m}} \right) \cdot [g_{17} \cdot \sin(\delta_{2,m} - \delta_{1,m}) - b_{17} \cdot \cos(\delta_{2,m} - \delta_{1,m})]$$

The Voltage Regulator (line 18):

$$f_{18,m}^{1,P} = g_{18} \cdot \left(\frac{V_{8,m}}{T_{VR,m}} \right)^2 - \left(\frac{V_{8,m}}{T_{VR,m}} \right) \cdot V_{9,m} \cdot [g_{18} \cdot \cos(\delta_{8,m} - \delta_{9,m}) + b_{18} \cdot \sin(\delta_{8,m} - \delta_{9,m})]$$

$$f_{18,m}^{1,Q} = -b_{18} \cdot \left(\frac{V_{8,m}}{T_{VR,m}} \right)^2 - \left(\frac{V_{8,m}}{T_{VR,m}} \right) \cdot V_{9,m} \cdot [g_{18} \cdot \sin(\delta_{8,m} - \delta_{9,m}) - b_{18} \cdot \cos(\delta_{8,m} - \delta_{9,m})]$$

$$f_{18,m}^{2,P} = g_{18} \cdot V_{9,m}^2 - V_{9,m} \cdot \left(\frac{V_{8,m}}{T_{VR,m}} \right) \cdot [g_{18} \cdot \cos(\delta_{9,m} - \delta_{8,m}) + b_{18} \cdot \sin(\delta_{9,m} - \delta_{8,m})]$$

$$f_{18,m}^{2,Q} = -b_{18} \cdot V_{9,m}^2 - V_{9,m} \cdot \left(\frac{V_{8,m}}{T_{VR,m}} \right) \cdot [g_{18} \cdot \sin(\delta_{9,m} - \delta_{8,m}) - b_{18} \cdot \cos(\delta_{9,m} - \delta_{8,m})]$$

ii. Constraints on external sources:

$$p_{x,m} = p_{slack\ bus,m} \ \& \ q_{x,m} \ is \ q_{slack\ bus,m}$$

$$p_{slack\ bus}^- = -60/MVA_{Base} \ ; \ q_{slack\ bus}^- = -60/MVA_{Base}$$

$$p_{slack\ bus}^+ = 60/MVA_{Base} \ ; \ q_{slack\ bus}^+ = 60/MVA_{Base}$$

$$p_{slack\ bus}^- \leq p_{slack\ bus,m} \leq p_{slack\ bus}^+$$

$$q_{slack\ bus}^- \leq q_{slack\ bus,m} \leq q_{slack\ bus}^+$$

iii. Power factor constraint:

For the case of PFC:

$$PF_{g,m} = \cos(\phi_{g,m}), PF_g^- = 0.95; PF_g^+ = 0.98; PF_g^- \leq PF_{g,m} \leq PF_g^+$$

iv. Thermal limit inequality constraints:

$\forall l \in L$ ($l=1$ to 18, $L=18$) & $\forall m \in M$ ($m = 1$ to 74, $M = 74$):

Apply equation (3-9) and equation (3-10).

v. Power balance equations at each bus:

$\forall m \in M$ ($m=1$ to 74), applying equation (3-17), Example:

At Bus 1:

$$p_{slack\ bus,m} = f_{16,m}^{1,P} + f_{17,m}^{1,P}; (p_{x,m} \text{ is } p_{slack\ bus,m})$$

At Bus 2:

$$-d_2^P \cdot \eta_m = f_{16,m}^{2,P} + f_{17,m}^{2,P} + f_{1,m}^{1,P} + f_{2,m}^{1,P} + f_{11,m}^{1,P} + f_{12,m}^{1,P}$$

.
.

.

At Bus 16:

No CVC & No curtailment	Capacitive	$p_{16}W_m - d_2^P \cdot \eta_m = f_{15,m}^{2,P}$
	Inductive	
CVC	Capacitive	$p_{16}W_m - p_{16,m}^{curt} - d_2^P \cdot \eta_m = f_{15,m}^{2,P}$
	Inductive	
CVC + Energy Curtailment	Capacitive	
	Inductive	

vi. Reactive power balance equations at each bus:

$\forall m \in M$ ($m = 1$ to 74);

At Bus 1:

$$q_{slack\ bus,m} = f_{16,m}^{1,Q} + f_{17,m}^{1,Q}; (q_{x,m} \text{ is } q_{slack\ bus,m})$$

At Bus 2:

$$Q_{2,m}^C - d_2^Q \cdot \eta_m = f_{16,m}^{2,Q} + f_{17,m}^{2,Q} + f_{1,m}^{1,Q} + f_{2,m}^{1,Q} + f_{11,m}^{1,Q} + f_{12,m}^{1,Q} - \frac{(V_{2,m})^2}{2} \cdot b_{12}^C$$

$$-\infty \leq Q_{2,m}^C \leq \infty$$

.
.

.

At Bus 9:

No CVC & No curtailment	Capacitive	$Q_{9,m}^C - d_9^Q \cdot \eta_m = f_{18,m}^{1,Q} + f_{18,m}^{2,Q}$ $-\infty \leq Q_{9,m}^C \leq \infty$
	Inductive	
CVC	Capacitive	$-d_9^Q \cdot \eta_m = f_{18,m}^{1,Q} + f_{18,m}^{2,Q}$
	Inductive	
CVC + Energy Curtailment	Capacitive	
	Inductive	

.
.

.

At Bus 16:

Depends on the case:

No CVC & No curtailment	Capacitive	$p_{16} \cdot w_m \cdot \tan(\phi_{16,m}) - d_{16}^Q \cdot \eta_m = f_{15,m}^{2,Q}$
	Inductive	$-p_{16} \cdot w_m \cdot \tan(\phi_{16,m}) - d_{16}^Q \cdot \eta_m = f_{15,m}^{2,Q}$
CVC	Capacitive	$p_{16} \cdot w_m \cdot \tan(\phi_{16,m}) - d_{16}^Q \cdot \eta_m = f_{15,m}^{2,Q}$
	Inductive	$-p_{16} \cdot w_m \cdot \tan(\phi_{16,m}) - d_{16}^Q \cdot \eta_m = f_{15,m}^{2,Q}$
CVC + Energy Curtailment	Capacitive	$p_{16} \cdot w_m \cdot \tan(\phi_{16,m}) - p_{16,m}^{curt} \cdot \tan(\phi_{16,m}) - d_{16}^Q \cdot \eta_m = f_{15,m}^{2,Q}$
	Inductive	$-[p_{16} \cdot w_m \cdot \tan(\phi_{16,m}) - p_{16,m}^{curt} \cdot \tan(\phi_{16,m})] - d_{16}^Q \cdot \eta_m = f_{15,m}^{2,Q}$

vii. Constraint on the power curtailed:

$\lambda_{curt} = 0.02$ or 0.05 or 0.1 , depending on the case.

$$\sum_{m \in M} p_{16,m}^{curt} \cdot \tau_m \leq \lambda_{curt} [\sum_{m \in M} p_{16} w_m \tau_m]$$

$$p_{16,m}^{curt} \leq p_{16} w_m$$

viii. Slack Bus Constraint:

$V_1 = 1$; “Slack Bus” and $\delta_{bo,m} = 0$;

ix. Voltage Limit Constraints:

$\forall m \in M (m=1 \text{ to } 74) \ \& \ (b = 3 \text{ to } 16, b \neq 2 \text{ and } b \neq 9);$

Applying equation (3-6), the exception is at the secondary of the OLTC and the VR as in the following table:

No CVC & No curtailment	Capacitive	$V_{2_{OLTC},m} = 1.036 \ \& \ V_{9_{VR},m} = 1.03$
	Inductive	
CVC	Capacitive	$V_{2_{OLTC}}^- = 0.94; V_{2_{OLTC}}^+ = 1.06 \Rightarrow$ $V_{2_{OLTC}}^- \leq V_{2_{OLTC},m} \leq V_{2_{OLTC}}^+$
	Inductive	
CVC + Energy Curtailment	Capacitive	$V_{9_{VR}}^- = 0.94; V_{9_{VR}}^+ = 1.06 \Rightarrow$ $V_{9_{VR}}^- \leq V_{9_{VR},m} \leq V_{9_{VR}}^+$
	Inductive	

x. Tapping Limit Constraints:

No CVC & No curtailment	Capacitive	$T_{OLTC,m} = 0.92 \ \& \ T_{VR,m} = 0.9$
	Inductive	
CVC	Capacitive	$0.85 \leq T_{OLTC,m} \leq 1.05$ $0.85 \leq T_{VR,m} \leq 1.05$
	Inductive	
CVC + Energy Curtailment	Capacitive	
	Inductive	

A.7: Unknown Variables

Different optimization software's will differ in the way the model is coded, any optimization software used will have to find the values of the following unknowns,.

$\forall m \in M (m=1 \text{ to } 74);$

i. Unknown voltage magnitude at each bus for each period:

$\forall m \in M (m=1 \text{ to } 74) \ \text{and} \ (\forall b \in B (b=2 \text{ to } 16)) \ \text{find} \ V_{b,m}, \ \text{So} :$

Unknown variables = $15 \times 74 = 1110$ variables

ii. Unknown angles magnitude at each bus for each period:

$\forall m \in M (m=1 \text{ to } 74) \ \text{and} \ (\forall b \in B (b=2 \text{ to } 16)) \ \text{find} \ \delta_{b,m}, \ \text{So} :$

Unknown variables = $15 \times 74 = 1110$ variables

iii. Unknown active power and reactive power flow on start/end of each line for each period:

Management of Active Distribution Networks with High Penetration of Distributed Generation

$\forall m \in M$ ($m=1$ to 74) and ($\forall l \in L$ ($l=1$ to 18)) find:

$$f_{b,m}^{1,P}, f_{b,m}^{1,Q}, f_{b,m}^{2,P}, f_{b,m}^{2,Q}$$

Unknown variables = $74 \times 18 \times 4 = 5328$ variables

- iv. Unknown active power/reactive power supplied from the Slack bus (external source) during each period:**

$$P_{slack\ bus,m}; Q_{slack\ bus,m}$$

Unknown variables = $2 \times 74 = 148$ variables

- v. Unknown active power curtailed from the wind turbine during each period:**

$$P_{16,m}^{curt}$$

Unknown variables = 74 variables

Unknown Tapping position of the OLTC and the VR:

$$T_{OLTC,m}; T_{VR,m}$$

Unknown variables = $2 \times 74 = 148$ variables

- vi. Unknown power factor and corresponding power angle at DG bus for each period:**

$$PF_{g,m}; \phi_{g,m}$$

Unknown variables = $2 \times 74 = 148$ variables

- vii. Unknown external reactive power support needed to balance the system for each period:**

$$Q_{2,m}^C$$

Unknown variables = 74 variables

(Hint: In case of passive management there is also $Q_{2,m}^C$ & $Q_{9,m}^C$ and in that case the Unknown variables = 148 variables.

- viii. Total Unknown Variables:**

Total unknown variables = $1110 + 1110 + 5328 + 148 + 74 + 148 + 148 + 74 = 8140$ unknown variable

References

- [1] Thomas Ackermann, Göran Andersson, and Lennart Söder, "Distributed generation: a definition," *Electric Power Systems Research*, vol. 57, pp. 195-204, 2001.
- [2] T. Ackermann, *Wind Power in Power Systems*: John Wiley & Sons, 2005.
- [3] CIGRE working group 37.23, "Impact of Increasing Contribution of Dispersed Generation on the Power System," Paris, France 1999.
- [4] S. N. Liew and G. Strbac, "Maximising penetration of wind generation in existing distribution networks," *IEE Proceedings - Generation, Transmission and Distribution*, vol. 149, pp. 256-262, 2002.
- [5] C. L. Masters, J. Mutale, G. Strbac, S. Curcic, and N. Jenkins, "Statistical evaluation of voltages in distribution systems with embedded wind generation," *IEE Proceedings - Generation, Transmission and Distribution*, vol. 147, pp. 207-212, 2000.
- [6] L. F. Ochoa, C. J. Dent, and G. P. Harrison, "Distribution Network Capacity Assessment: Variable DG and Active Networks," *IEEE Transactions on Power Systems*, vol. 25, pp. 87-95, 2010.
- [7] R. A. F. Currie, G. W. Ault, R. W. Fordyce, D. F. MacLeman, M. Smith, and J. R. McDonald, "Actively Managing Wind Farm Power Output," *IEEE Transactions on Power Systems*, vol. 23, pp. 1523-1524, 2008.
- [8] EA Technology, "A Technical Review and Assessment of Active Network Management Infrastructures and Practices," U.K. Department of Trade and Industry (DTI), April 2006.
- [9] J. McDonald, "Leader or follower [The Business Scene]," *IEEE Power and Energy Magazine*, vol. 6, pp. 18-90, 2008.
- [10] G. W. Ault, R. A. F. Currie, and J. R. McDonald, "Active power flow management solutions for maximising DG connection capacity," in *IEEE Power Engineering Society General Meeting, 2006*, 2006, p. 5 pp.
- [11] P. Djapic, C. Ramsay, D. Pudjianto, G. Strbac, J. Mutale, N. Jenkins, *et al.*, "Taking an active approach," *IEEE Power and Energy Magazine*, vol. 5, pp. 68-77, 2007.
- [12] Jim McDonald, "Adaptive intelligent power systems: Active distribution networks," *Energy Policy*, vol. 36, pp. 4346-4351, 2008.
- [13] P. Chiradeja and R. Ramakumar, "An approach to quantify the technical benefits of distributed generation," *IEEE Transactions on Energy Conversion*, vol. 19, pp. 764-773, 2004.
- [14] L. F. Ochoa, A. Padilha-Feltrin, and G. P. Harrison, "Evaluating distributed generation impacts with a multiobjective index," *IEEE Transactions on Power Delivery*, vol. 21, pp. 1452-1458, 2006.
- [15] D. Singh and R. K. Misra, "Effect of Load Models in Distributed Generation Planning," *IEEE Transactions on Power Systems*, vol. 22, pp. 2204-2212, 2007.
- [16] L. F. Ochoa, A. Padilha-Feltrin, and G. P. Harrison, "Evaluating Distributed Time-Varying Generation Through a Multiobjective Index," *IEEE Transactions on Power Delivery*, vol. 23, pp. 1132-1138, 2008.

- [17] Wang Caisheng and M. H. Nehrir, "Analytical approaches for optimal placement of distributed generation sources in power systems," in *IEEE Power Engineering Society General Meeting*, 2005, p. 2393 Vol. 3.
- [18] Naresh Acharya, Pukar Mahat, and N. Mithulananthan, "An analytical approach for DG allocation in primary distribution network," *International Journal of Electrical Power & Energy Systems*, vol. 28, pp. 669-678, 2006.
- [19] A. Silvestri, A. Berizzi, and S. Buonanno, "Distributed generation planning using genetic algorithms," in *Electric Power Engineering, 1999. PowerTech Budapest 99. International Conference on*, 1999, p. 257.
- [20] G. Celli, E. Ghiani, S. Mocci, and F. Pilo, "A multiobjective evolutionary algorithm for the sizing and siting of distributed generation," *IEEE Transactions on Power Systems*, vol. 20, pp. 750-757, 2005.
- [21] L. F. Ochoa, A. Padilha-Feltrin, and G. P. Harrison, "Time-Series-Based Maximization of Distributed Wind Power Generation Integration," *IEEE Transactions on Energy Conversion*, vol. 23, pp. 968-974, 2008.
- [22] A. Keane and M. O'Malley, "Optimal Utilization of Distribution Networks for Energy Harvesting," *IEEE Transactions on Power Systems*, vol. 22, pp. 467-475, 2007.
- [23] G. P. Harrison and A. R. Wallace, "Optimal power flow evaluation of distribution network capacity for the connection of distributed generation," *IEE Proceedings - Generation, Transmission and Distribution*, vol. 152, pp. 115-122, 2005.
- [24] C. J. Dent, L. F. Ochoa, and G. P. Harrison, "Network distributed generation capacity analysis using OPF with voltage step constraints," in *Electricity Distribution - Part 1, 2009. CIRED 2009. 20th International Conference and Exhibition on*, 2009, pp. 1-4.
- [25] C. J. Dent, L. F. Ochoa, G. P. Harrison, and J. W. Bialek, "Efficient Secure AC OPF for Network Generation Capacity Assessment," *IEEE Transactions on Power Systems*, vol. 25, pp. 575-583, 2010.
- [26] N. S. Rau and Wan Yih-Heui, "Optimum location of resources in distributed planning," *IEEE Transactions on Power Systems*, vol. 9, pp. 2014-2020, 1994.
- [27] P. N. Vovos and J. W. Bialek, "Direct incorporation of fault level constraints in optimal power flow as a tool for network capacity analysis," *IEEE Transactions on Power Systems*, vol. 20, pp. 2125-2134, 2005.
- [28] T. Boehme, A. R. Wallace, and G. P. Harrison, "Applying Time Series to Power Flow Analysis in Networks With High Wind Penetration," *Power Systems, IEEE Transactions on*, vol. 22, pp. 951-957, 2007.
- [29] P. N. Vovos, A. E. Kiprakis, A. R. Wallace, and G. P. Harrison, "Centralized and Distributed Voltage Control: Impact on Distributed Generation Penetration," *IEEE Transactions on Power Systems*, vol. 22, pp. 476-483, 2007.
- [30] L. F. Ochoa, C. J. Dent, and G. P. Harrison, "Maximisation of intermittent distributed generation in active networks," in *IET-CIRED Seminar on SmartGrids for Distribution*, 2008, pp. 1-4.
- [31] S. Civanlar, J. J. Grainger, H. Yin, and S. S. H. Lee, "Distribution feeder reconfiguration for loss reduction," *IEEE Transactions on Power Delivery*, vol. 3, pp. 1217-1223, 1988.

- [32] D. Shirmohammadi and H. W. Hong, "Reconfiguration of electric distribution networks for resistive line losses reduction," *IEEE Transactions on Power Delivery*, vol. 4, pp. 1492-1498, 1989.
- [33] M. E. Baran and F. F. Wu, "Optimal capacitor placement on radial distribution systems," *IEEE Transactions on Power Delivery*, vol. 4, pp. 725-734, 1989.
- [34] Luis F. Ochoa, Andrew Keane, Chris Dent, and Gareth P. Harrison, "Applying active network management schemes to an Irish distribution network for wind power maximisation," in *Electricity Distribution - Part 1, 2009. CIRED 2009. 20th International Conference and Exhibition on*, 2009, pp. 1-4.
- [35] L. F. Ochoa and G. P. Harrison, "Minimizing Energy Losses: Optimal Accommodation and Smart Operation of Renewable Distributed Generation," *IEEE Transactions on Power Systems*, vol. 26, pp. 198-205, 2011.
- [36] Vladimir Stanojevic, Vera Silva, Danny Pudjianto, Goran Strbac, Peter Lang, and David Macleaman, "Application of storage and Demand Side Management to optimise existing network capacity," in *Electricity Distribution - Part 1, 2009. CIRED 2009. 20th International Conference and Exhibition on*, 2009, pp. 1-4.
- [37] Available: <http://www.lindo.com/>
- [38] McDonald Jim, "Adaptive intelligent power systems: Active distribution networks," *Energy Policy*, vol. 36, pp. 4346-4351, 2008.
- [39] T. Gönen, *Electric power distribution system engineering*: McGraw-Hill, 1986.
- [40] T.A. Short, *Electric Power Distribution Handbook*: CRC Press, 2004.
- [41] P. Siano, P. Chen, Z. Chen, and A. Piccolo, "Evaluating maximum wind energy exploitation in active distribution networks," *IET Generation, Transmission & Distribution*, vol. 4, pp. 598-608, 2010.
- [42] G. Celli, E. Ghiani, S. Mocci, F. Pilo, and E. Pazzola, "Demand Side Management as a support to distributed generation in active networks," in *Electricity Distribution, 2005. CIRED 2005. 18th International Conference and Exhibition on*, 2005, pp. 1-4.
- [43] C. Schwaegerl, M. H. J. Bollen, K. Karoui, and A. Yagmur, "Voltage control in distribution systems as a limitation of the hosting capacity for distributed energy resources," in *Electricity Distribution, 2005. CIRED 2005. 18th International Conference and Exhibition on*, 2005, pp. 1-5.
- [44] T.H. Boehme, *Matching renewable electricity generation with demand in Scotland*: University of Edinburgh, 2006.
- [45] distributed generation sustainable electrical energy centre. Available: <http://www.sedg.ac.uk/>
- [46] L. F. Ochoa and G. P. Harrison, "Using AC Optimal Power Flow for DG planning and optimisation," in *IEEE Power and Energy Society General Meeting 2010*, pp. 1-7.